Supporting Information

Single-atom engineering of hemicyanine and its amphiphilic derivative for optimized near infrared phototheranostics

ShanKun Yao,[a,b] Yuncong Chen,[*a,b,c] Weizhong Ding,[a] Fengwu Xu,[a] Zhipeng Liu,[a] Yaheng Li,[a] Yanping Wu,[a] Shumeng Li,[a] Weijiang He,[a,c] and Zijian Guo,[*a,b,c]

a. State Key Laboratory of Coordination Chemistry, Coordination Chemistry Institute, School of Chemistry and Chemical Engineering, Nanjing University, Nanjing 210023, P.R. China
E-mail: chenyc@nju.edu.cn; zguo@nju.edu.cn

b. Chemistry and Biomedicine Innovation Center (ChemBIC), Nanjing University, Nanjing 210023, P. R. China

c. Nanchuang (Jiangsu) Institute of Chemistry and Health, Jiangsu, Nanjing 210000, P.R. China

d. College of Materials Science and Engineering, Nanjing Forestry University, Nanjing, 210037, P. R. China

Contents

General experimental procedures

S1. Materials and instruments

All reagents for CyX-NEt_2 (X= O, S, Se) preparation were of analytic grade and purchased from Energy Chemistry and J&K Chemical. The ^{1}H NMR and ^{13}C NMR spectra were recorded at 25℃ with a Bruker Avance DRX-400 with TMS as the internal reference. High resolution mass spectrometric data were determined using an Agilent 6540Q-TOF HPLC-MS spectrometer. Solvents for spectroscopic study were of spectral grade from Tedia Company Inc. The ultrapure water for spectroscopic and cell culture was obtained from Millipore system (>18.2 MΩ). Fluorescence spectra were determined using a Horiba FluoroMax-4 spectrofluorometer with a 4 nm slit for both excitation and emission. Absorption spectra were recorded using a Perkin Elmer E35 spectrophotometer. Particle size was measured by dynamic light scattering (DLS) on Zetasizer Nanoseries (Nano ZS90). Isoflurane for in vivo imaging was purchased from RWD Life Science. An IVIS Lumina K Series III instrument (PerkinElmer) was used for optical imaging, and image analysis was realized with Living Image 4.5. Photothermal images were measured by NIR thermal imager (FLIR E40).Confocal imaging was performed with Leica SP8 STED 3X and Zeiss LSM710 microscope.

S2. Synthesis

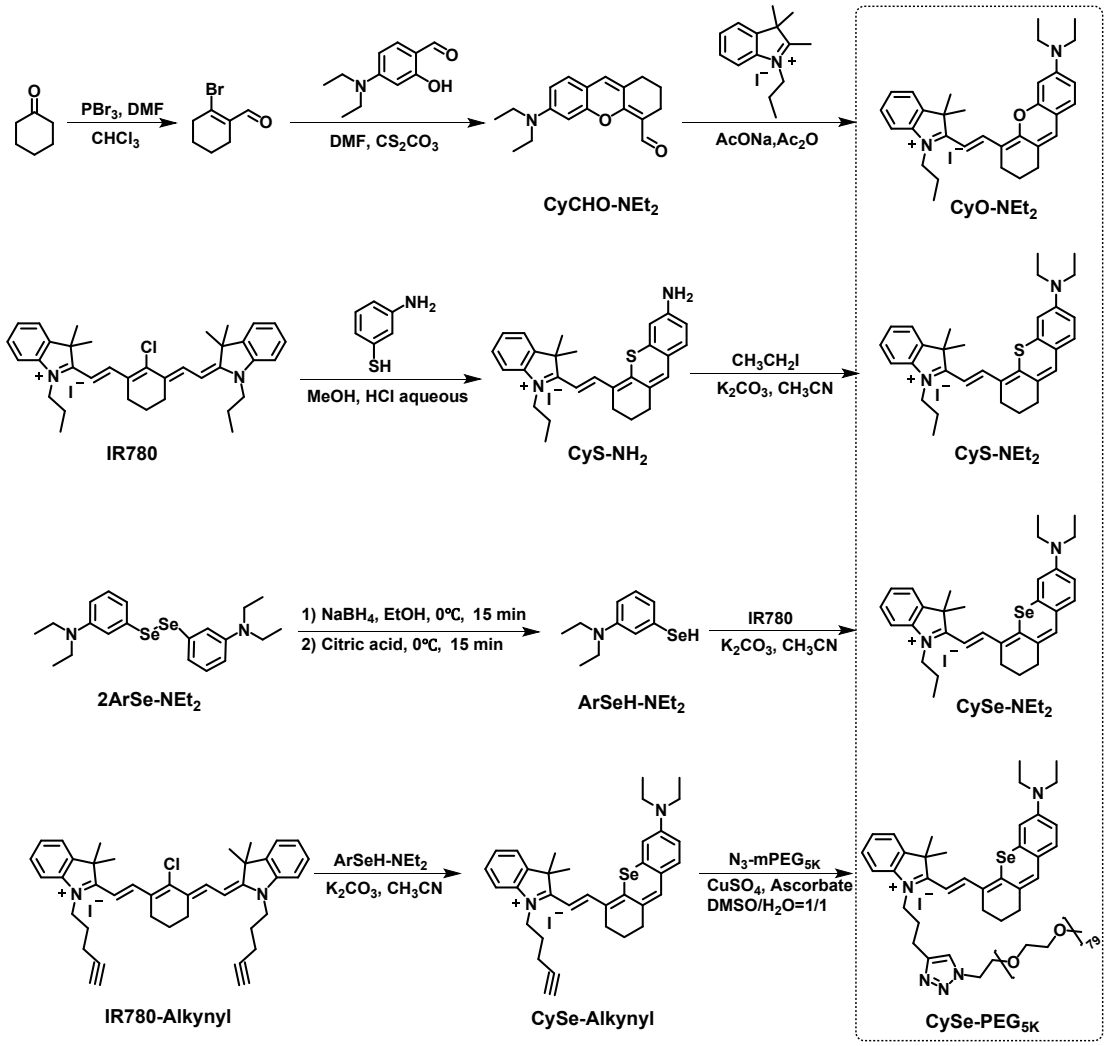

Scheme S1. Synthetic routes and chemical structures of hemicyanine photosensitizers, that is, CyO-NEt_2, CyS-NEt_2, **CySe-NEt_2** and **CySe-mPEG$_{5K}$**.

Compounds CyCHO-NEt_2, CyS-NH_2, 2ArSe-NEt_2, IR780-Alkynyl and were prepared according to the literature procedures [1-5].

CyCHO-NEt_2: ^{1}H NMR (400 MHz, $CDCl_3$): δ 10.29 (s, 1H), 7.00 (d, *J* = 8.6 Hz, 1H), 6.62 (s, 1H), 6.42 (d, *J* = 8.7 Hz, 1H), 6.37 (s, 1H), 3.39 (q, *J* = 7.1 Hz, 4H), 2.54 (td, *J* = 6.7, 1.5 Hz, 2H), 2.45 (t, *J* = 6.1 Hz, 2H), 1.76-1.64 (m, 2H), 1.20 (t, *J* = 7.1 Hz, 6H) ppm.

CyS-NH_2: ^{1}H NMR (400 MHz, methanol-d_4) δ 8.32 (d, *J* = 13.8 Hz, 1H), 7.61 (d, *J* = 7.4 Hz, 1H), 7.49 (dd, *J* = 7.9, 4.2 Hz, 2H), 7.43 (d, *J* = 8.9 Hz, 2H), 7.37 (t, *J* = 7.4 Hz, 1H), 6.93 (d, *J* = 1.8 Hz, 1H), 6.87 (dd, *J* = 8.6, 2.1 Hz, 1H), 6.39 (d, *J* = 13.8 Hz, 1H), 4.22 (t, *J* = 7.3 Hz, 2H), 2.92-2.77 (m, 2H), 2.71 (t, *J* = 6.1 Hz, 2H), 2.04-1.86 (m, 4H), 1.79 (s, 6H), 1.08 (t, *J* = 7.4 Hz, 3H) ppm.

2ArSe-NEt_2: ^{1}H NMR (400 MHz, $CDCl_3$): δ 7.09 (t, *J* = 7.9 Hz, 2H), 6.98 (d, *J* = 24.9 Hz, 2H), 6.92 (d, *J* = 7.3 Hz, 2H), 6.54 (d, *J* = 7.5 Hz, 2H), 3.30 (q, *J* = 7.0 Hz, 8H), 1.12 (t, *J* = 7.1 Hz, 12H) ppm.

IR780-Alkynyl: ^{1}H NMR (400 MHz, $CDCl_3$): δ 8.37 (d, *J* = 14.1 Hz, 2H), 7.45-7.38 (m, 4H), 7.34 (d, *J* = 7.8 Hz, 2H), 7.30-7.23 (m, 2H), 6.35 (d, *J* = 14.1 Hz, 2H), 4.37 (t, *J* = 7.3 Hz, 4H), 2.77 (t, *J* = 6.1 Hz, 4H), 2.47 (td, *J* = 6.6, 2.5 Hz, 4H), 2.16-2.05 (m, 6H), 2.03-1.92 (m, 2H), 1.74 (s, 12H) ppm.

S2.1 Synthesis of **ArSeH-NEt_2**

$NaBH_4$ (23 mg, 0.6 mmol) was added portionwise to a stirred solution of 2ArSe-NEt_2 (91 mg, 0.2 mmol) in EtOH (2 mL) at 0 ℃ under N_2 atmosphere. After 15 minutes, solid citric acid (192 mg, 1.0 mmol) was added and the reaction mixture was stirred at 0 °C for 5 minutes. The mixture was then diluted with Et_2O (5 mL) and H_2O (3 mL) was added. The layers were separated and the organic layer was washed with saturated aqueous solution NH_4Cl (2 mL) and brine (2 mL), dried over Na_2SO_4, filtered and concentrated in vacuo to give ArSeH-NEt_2 without further purification. ^{1}H NMR (400 MHz, $CDCl_3$): δ 7.09 (t, *J* = 7.9 Hz, 1H), 6.97-6.88 (m, 2H), 6.54 (d, *J* = 7.5 Hz, 1H), 3.30 (q, *J* = 7.0 Hz, 4H), 1.12 (t, *J* = 7.1 Hz, 6H) ppm.

S2.2 Synthesis of **CyO-NEt_2**

CyCHO-NEt_2 (280 mg, 1.0 mmol), CH_3COONa (164 mg, 2.0 mmol) and compound 3 (395 g, 1.2 mmol) were dissolved in anhydrous Ac_2O (25 mL). The mixture was stirred at 25°C for 18 hours. The resulting dark green solution was concentrated and the resulting residue was dissolved in CH_2Cl_2, then washed three times with water and dried over Na_2SO_4. The solvent was evaporated under reduced pressure and the residue was purified by silica gel chromatographed using CH_2Cl_2/CH_3OH (100/3, v/v)

as eluent to give the product as a dark green solid. Yield: 0.38 g (65%). ^{1}H NMR (400 MHz, CD_2Cl_2): δ 8.54 (d, *J* = 14.2 Hz, 1H), 7.53-7.40 (m, 4H), 7.30 (td, *J* = 7.5, 0.7 Hz, 1H), 7.21 (d, *J* = 7.9 Hz, 1H), 6.84 (dd, *J* = 9.0, 2.4 Hz, 1H), 6.55 (d, *J* = 2.0 Hz, 1H), 6.08 (d, *J* = 14.2 Hz, 1H), 4.07 (t, *J* = 7.5 Hz, 2H), 3.55 (q, *J* = 7.1 Hz, 4H), 2.78 (t, *J* = 6.1 Hz, 2H), 2.69 (t, *J* = 6.1 Hz, 2H), 1.99-1.86 (m, 4H), 1.77 (s, 6H), 1.29 (t, *J* = 7.1 Hz, 6H), 1.09 (t, *J* = 7.4 Hz, 3H) ppm. ^{13}C NMR (100 MHz, CD_2Cl_2): δ 174.69, 165.12, 157.78, 153.62, 143.64, 143.45, 142.16, 139.94, 130.94, 130.06, 126.67, 124.63, 123.67, 116.38, 114.51, 113.79, 112.22, 100.72, 97.02, 55.21, 50.78, 47.49, 46.58, 30.04, 29.63, 25.81, 22.03, 13.59, 12.71 ppm. HR-MS (ESI, positive mode, *m/z*): calcd. 467.30569, found 467.30423 for $[M-I]^+$.

S2.3 Synthesis of **CyS-NEt$_2$**

To a stirred solution of compound CyS-NH_2 (200 mg, 0.361 mmol) in CH_3CN (30 mL) at 0 ℃ under N_2 atmosphere, iodoethane (281 mg, 1.8 mmol) and K_2CO_3 (200 mg, 1.44 mmol) were added and the solution was refluxed at 85 ℃ for 18 h. The reaction solvent was removed and diluted with CH_2Cl_2, then washed with pure water, the organic layer was dried over sodium sulfate anhydrous and concentrated under reduced pressure. The residue was separated by column chromatography using CH_2Cl_2:CH_3OH (v/v, 50:1) as eluent, obtaining the blue-green solid product, yield 15%. ^{1}H NMR (400 MHz, CD_2Cl_2): δ 8.24 (d, *J* = 13.6 Hz, 1H), 7.51 (dd, *J* = 14.8, 8.1 Hz, 2H), 7.43 (dd, *J* = 16.9, 9.2 Hz, 2H), 7.32 (t, *J* = 7.4 Hz, 1H), 7.21 (d, *J* = 7.9 Hz, 1H), 6.92 (d, *J* = 10.5 Hz, 2H), 6.17 (d, *J* = 13.7 Hz, 1H), 4.06 (t, *J* = 7.3 Hz, 2H), 3.53 (dd, *J* = 13.9, 6.9 Hz, 4H), 2.79 (t, *J* = 5.8 Hz, 2H), 2.67 (t, *J* = 5.8 Hz, 2H), 2.06-1.87 (m, 4H), 1.79 (s, 6H), 1.28 (t, *J* = 6.9 Hz, 6H), 1.07 (t, *J* = 7.3 Hz, 3H) ppm. ^{13}C NMR (100 MHz, CD_2Cl_2): δ 174.67, 159.09, 151.10, 143.29, 142.46, 141.96, 140.66, 134.71, 131.68, 130.12, 126.90, 126.58, 123.78, 120.75, 115.91, 112.34, 106.16, 101.97, 97.33, 50.91, 47.50, 46.45, 33.66, 29.94, 28.03, 22.10, 22.04, 13.68, 12.70 ppm. HR-MS (ESI, positive mode, *m/z*): calcd. 483.28284, found 483.28107 for $[M-I]^+$.

S2.4 Synthesis of **CySe-NEt$_2$**

ArSeH-NEt_2 (361 mg, 1.58 mmol), K_2CO_3 (218 mg, 1.58 mmol) and IR780 (700 mg, 1.05 mmol) and were dissolved in 30 mL CH_3CN solvent in a flask, and the mixture was stirred and refluxed for 24 hours under argon atmosphere. After completed, the crude product was obtained by rotary distillation under reduced pressure, and was purified by silica gel column chromatography using CH_2Cl_2:CH_3OH (v/v, 94:4) as an eluent to get blue-green powder, yield 20%. ^{1}H NMR (400 MHz, CD_2Cl_2): δ 8.08 (d, *J* = 13.7 Hz, 1H), 7.53 (d, *J* = 8.6 Hz, 2H), 7.46 (t, *J* = 7.6 Hz, 1H), 7.36 (t, *J* = 7.4 Hz, 1H), 7.30-7.24 (m, 2H), 7.04 (d, *J* = 1.9 Hz, 1H), 6.85 (d, *J* = 9.0 Hz, 1H), 6.30 (d, *J* = 13.7 Hz, 1H), 4.12 (t, *J* = 7.4 Hz, 2H), 3.51 (q, *J* = 7.0 Hz, 4H), 2.81 (t, *J* = 6.0 Hz, 2H)), 2.66 (t, *J* = 6.0 Hz, 2H), 2.03-1.84 (m, 4H), 1.79 (s, 6H), 1.27 (t, *J* = 7.0 Hz, 6H), 1.07 (t, *J* = 7.3 Hz, 3H) ppm. ^{13}C NMR (100 MHz, CD_2Cl_2): δ 174.36, 161.53, 149.46, 144.40, 142.03, 141.59, 141.36, 139.08, 134.76, 130.56, 128.92, 128.75, 126.09, 122.57, 120.03, 113.91, 111.47, 107.59, 102.26, 49.95, 46.52, 45.07, 33.43, 28.51, 27.56, 21.03, 20.91, 12.37, 11.37 ppm. HR-MS (ESI, positive mode, m/z): calcd. 531.22730, found 531.22687 for $[M-I]^+$.

S2.5 Synthesis of **CySe-Alkynyl**

ArSeH-NEt_2 (80 mg, 0.35 mmol), K_2CO_3 (48 mg, 0.35 mmol) and IR780-Alkynyl (166 mg, 0.23 mmol) and were dissolved in 30 mL CH_3CN solvent in a flask, and the mixture was stirred and refluxed for 24 hours under argon atmosphere. After completed, the crude product was obtained by rotary distillation under reduced pressure, and was purified by silica gel column chromatography using CH_2Cl_2:CH_3OH (v/v, 94:4) as an eluent to get blue-green powder, yield 25%. ^{1}H NMR (400 MHz, CD_2Cl_2): δ 8.07 (d, *J* = 13.6 Hz, 1H), 7.53 (dd, *J* = 12.0, 8.5 Hz, 2H), 7.45 (d, *J* = 7.5 Hz, 1H), 7.36 (dd, *J* = 16.4, 8.0 Hz, 2H), 7.28 (s, 1H), 7.01 (s, 1H), 6.86 (d, *J* = 8.6 Hz, 1H), 6.45 (d, *J* = 13.6 Hz, 1H), 4.34 (t, *J* = 7.1 Hz, 2H), 3.51 (dd, *J* = 13.7, 6.7 Hz, 4H), 2.80 (d, *J* = 4.7 Hz, 2H), 2.69 (d, *J* = 5.4 Hz, 2H), 2.44 (s, 2H), 2.22 (s, 1H), 2.13-2.04 (m, 2H), 1.98-1.92 (m, 2H), 1.78 (s, 6H), 1.27 (t, *J* = 6.8 Hz, 6H) ppm. ^{13}C NMR (100 MHz, CD_2Cl_2): δ 174.56, 162.10, 149.90, 144.94, 144.78, 142.24, 141.67, 139.70, 135.28, 131.16, 129.55, 129.38, 126.40, 122.90, 120.52, 114.41, 111.86, 107.90, 102.71, 83.21, 70.47, 50.24, 45.48, 43.93, 33.84, 28.91, 27.98, 26.49, 21.42, 16.38, 12.77 ppm. HR-MS (ESI, positive mode, m/z): calcd. 555.22730, found 555.22601 for $[M-I]^+$.

S2.6 Synthesis of **CySe-mPEG$_{5K}$**

CySe-mPEG$_{5K}$ was obtained by using copper(I)-catalyzed alkyne-azide cycloaddition (CAAC) reaction. CySe-Alkynyl (20 mg, 0.029 mmol), $CuSO_4 \cdot 5H_2O$ (7.33 mg, 0.029 mmol), sodium ascorbate (11.62 mg, 0.058 mmol), and N_3-mPEG-methoxy (M_n=5000) (155 mg, 0.029 mmol) were dissolved into DMSO/H_2O (5/5 mL). The reaction mixture was stirred under nitrogen atmosphere at room temperature overnight. Then the reaction solution was dialyzed against deionized water for 24 h to remove salts, N_3-mPEG-methoxy and DMSO, and freeze-dried to get CySe-mPEG$_{5K}$ with a yield of 95%. ^{1}H NMR (400 MHz, MeOD): δ 8.18 (d, *J* = 13.3 Hz, 1H), 7.69-7.61 (m, 3H), 7.57-7.48 (m, 2H), 7.45-7.39 (m, 2H), 7.26 (s, 1H), 6.99 (d, *J* = 7.8 Hz, 1H), 6.49 (d, *J* = 13.7 Hz, 1H), 4.62 (s, 2H), 4.38 (s, 2H), 4.15 (s, 2H), 4.06-3.54 (m, mPEG), 3.50 (dd, *J* = 9.3, 4.5 Hz, 4H), 3.40 (s, 3H), 3.27 (d, *J* = 5.0 Hz, 2H), 2.87 (s, 2H), 2.70 (s, 2H), 2.33 (s, 2H), 2.01 (s, 2H), 1.82 (s, 6H), 1.30 (t, *J* = 6.9 Hz, 6H) ppm. Modi-TOF-MS, *m/z*: found 5000~6000.

S3. Spectroscopic study

Detection of fluorescence quantum yield: The fluorescence quantum yield (QY) was determined according to following equation:

$$\phi_{sample} = \phi_{ICG} \times \frac{I^{sample} A^{ICG}}{I^{ICG} A^{sample}} \times [\frac{\eta^{sample}}{\eta^{ICG}}]^2$$

where Φ_{ICG} was the QY of reference, I was the area under the emission spectra, A was the absorbance at the excitation wavelength, and η was the refractive index of the used solvent. “sample” and “ICG” stand for compounds and reference, respectively. The fluorescence quantum yield were determined by measuring emission spectrum with ICG in DMSO (Φ_F = 0.13) as a reference, and the absorbance at the respective excitation wavelengths was controlled to be lower than 0.05.

The laser power density was determined according to following equation:

Laser power density (mW/cm^2) = Output power (mW) / Area of the spot (cm^2)

Where the “Output power” could be read from the 750 nm laser, and the “Area of the spot” was the beam area which could be calculated based on the equation “$\pi*D^2/4$” (here D is beam diameter).

Singlet oxygen ($^1O_2$) production: The singlet oxygen quantum yield (Φ_Δ) was determined according to following equation:

$$\phi_\Delta(^1O_2)^{sample} = \phi_\Delta(^1O_2)^{ICG}\frac{S^{sample}F^{ICG}}{S^{ICG}F^{sample}}$$

where “sample” and “ICG” stand for the compounds and the reference, respectively. S was the slope of the change in absorbance of DPBF at the absorbance maxima with the irradiation time (750 nm, 5 mW/cm^2). F is the absorption correction factor, which is given as F = 1-10^{-OD}.

Photoacoustic signal: The linear relationship of concentration vs PA signal intensity of CySe-mPEG$_{5k}$ in PBS was acquired by a point-to-point way. Briefly, the change of PA signal intensity at 775 nm with various concentrations of CySe-mPEG$_{5k}$ in PBS was measured by recording region of interest (ROI) analysis, respectively.

Photothermal effect: Infrared thermal imaging system was used for recording the temperature change of CySe-mPEG$_{5k}$ solution. Concentration-dependent experiment: 200 μL CySe-mPEG$_{5k}$ solution with various concentrations (20, 40 and 60 μM) in PBS were irradiated with a NIR laser (750 nm, 500 mW/cm^2). Power-dependent experiment: CySe-mPEG$_{5k}$ (200 μL, 60 μM) solution were irradiated with various NIR laser powers (200, 300 and 500 mW/cm^2) in PBS. Then the temperature changes were recorded, respectively. At last, the photothermal conversion efficiency of CyX-NEt$_2$ (X= O, S, Se) and CySe-mPEG$_{5k}$ was acquired referring to previous work [6-7].

S4. Cell experiment

Cell incubation: 4T1 cells were cultured in Dulbecco’s modified Eagle's medium (DMEM, Gibco) supplemented with 10% fetal bovine serum (FBS; Gibco) and glutamine (2 mM) in an atmosphere of 5% CO_2 and 95% air at 37°C.

Cell imaging: Co-localization experiments were investigated by co-incubation of CyX-NEt_2 (X= O, S, Se) (2.0 μM) and various commercial dyes (Mito-tracker green, Lyso-Tracker Green and DAPI) to the cells for 30 min, respectively, and then fluorescence images were acquired by using fluorescence microscope (Leica SP8 STED 3X). For **intracellular ROS detection**, 4T1 cells were seeded at confocal culture dishes and pre-incubated for 24 h. Then, 4.0 μM concentration of CyX-NEt_2/CySe-$mPEG_{5K}$ and 10 μM DCFH-DA were added and incubated for 30 min/3h, then, the cells were washed with PBS for 3 times and irradiation with 750 nm laser for 5 min and scanned under confocal microscopy at 488 nm excitation, whereas, the fluorescent channel at 500-550 nm was collected (N=3). For **live/dead cells assay**, cells were seeded in three confocal culture dishes at same density for 24 h incubation, 4.0 μM CySe-$mPEG_{5K}$ was added to the cell medium and incubated for another 3 h, then irradiated by 750 nm laser (500 mW/cm^2) for 5 min. The cells were incubated for another 24 h and then stained with calcein AM and propidium iodide (PI) for 30 min, washed with PBS, and then imaged by fluorescence microscope.

Cell cytotoxicity assay: 4T1 cells were plated ($4.5x10^4$ cells/well) in a 24-well plate in fetal bovine serum (10% FBS) media for 24 h. 4T1 cells were then incubated with different concentrations of CyX-NEt_2/CySe-$mPEG_{5K}$ at 37 °C in incubator. Then the plate was irradiated with 750 nm light at an average optical density and then incubated in for 24 h. As for the dark group, the cells were kept out of light with the other treatments unchanged. After 24 h, media was replaced with 2.5 mg/mL MTT reagent in PBS, and incubated for 3 h at 37 °C. Cells were then lysed using 150 μL DMSO, transferred to a 96-well plate and absorbances were measured using a plate reader at 490 nm. The absorbance at 490 nm was recorded by a microplate reader to calculate the cell viability from the following formula:

Cell viability (%) = (Mean absorbance of pretreated cells-Mean absorbance of blank medium) / (Mean absorbance of untreated cells-Mean absorbance of blank medium) × 100%

S5. Animal experiment

All of 4T1 xenograft tumor-bearing BALB/c mice were anesthetized by inhalation of isoflurane before injection and during imaging.

In/ex vivo fluorescence imaging of mice: Fluorescence imaging were obtained by an IVIS Lumina K Series III instrument (PerkinElmer) using excitation at 760 nm and collect bandpath of 825±20 nm. Upon intravenous injection of CySe-NEt_2 or CySe-$mPEG_{5K}$ (100 μL, 100 μM μM, in PBS), and fluorescence imaging was taken 0, 0.5, 1.0, 1.5, 2.0, 2.5, 3.0 and 4.0 h post injection. The mice were sacrificed by CO_2 exposure, then tumors and other organs were dissected and photographed by fluorescence imaging system.

In vivo photothermal imaging: Thermal imaging was performed with the American FLIR infrared thermal imaging equipment. PBS, CySe-NEt_2 or CySe-$mPEG_{5K}$ (200 μM, 100 μL) was injected into the tumor-bearing mice via the tail vein. After 1.0 hours, a 500 mW/cm^2 750 nm laser was used to illuminate the tumor area and record the temperature of the tumor area.

In vivo PA imaging: 4T1 xenograft tumor-bearing BALB/c mice were anesthetized by inhalation of isoflurane, followed by scanning on an animal photoacoustic imaging system (PA/US Vevo LAZR-X Fujifilm VisualSonics). After obtaining the background PA images, the mice were intravenously injected CySe-NEt_2 or CySe-$mPEG_{5K}$ in PBS. Then, PA signals of the tumor site at different post-injection time points (0, 1, 2, 3 and 4 h) were detected at an excitation wavelength of 780 nm.

In vivo antitumor studies: When the tumour volume reached to 80-100 mm^3, the 4T1 xenograft tumour mice were randomly divided into 3 groups (PBS, CySe-NEt_2, CySe-$mPEG_{5K}$, 200 μM, 100 μL in PBS, with or without laser N=5). The power density of 750 nm laser for PTT/PDT was 500 mW/cm^2 and the exposure time was 10 min. During therapy, the tumor volumes and body weights were measured every two days. The mice were sacrificed till 14 days posttreatment according to institutional guidelines. Tumors were resected, weighed, fixed in formalin and embedded in paraffin.

Results and Discussion

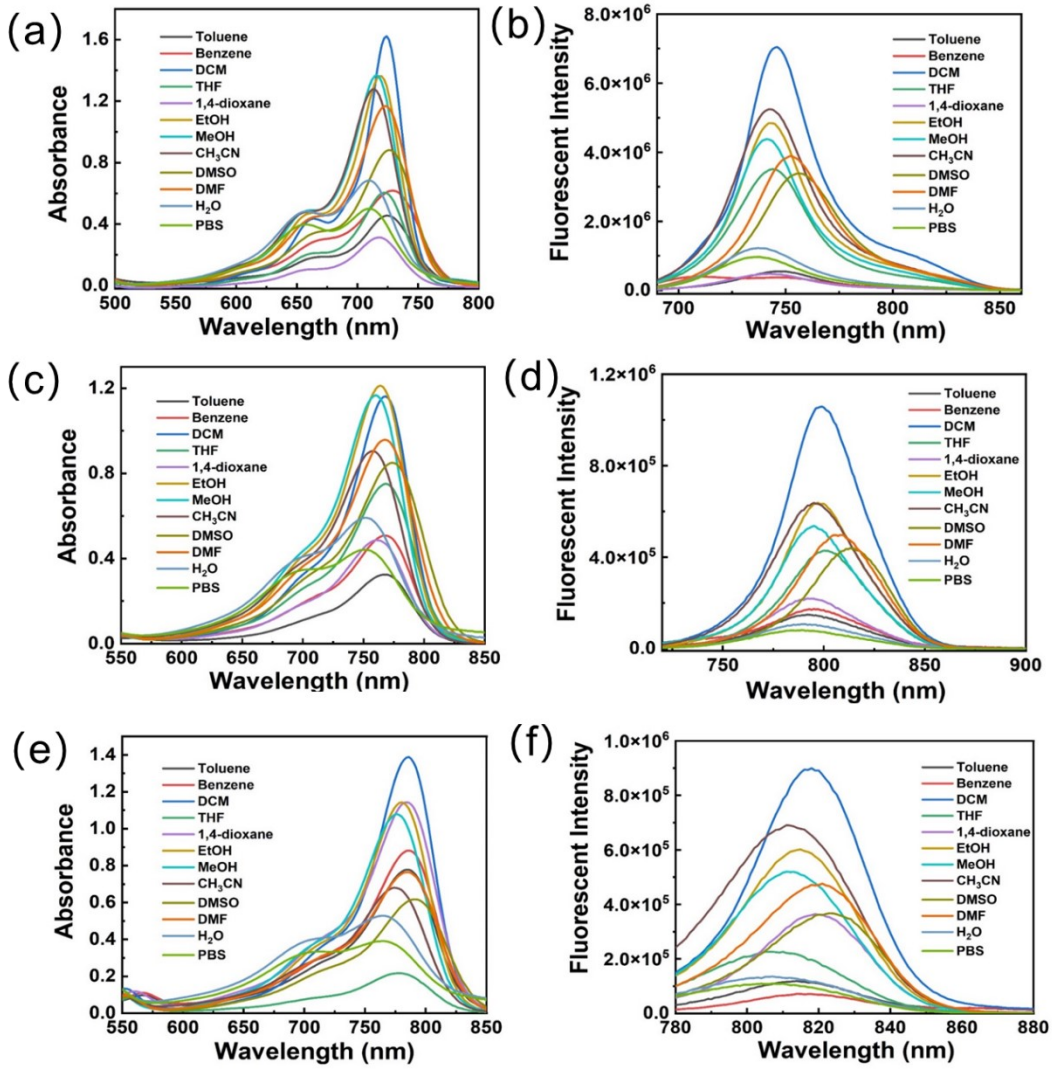

Figure S1. Absorption spectras of (a) CyO-NEt_2, (c) CyS-NEt_2 and (e) CySe-NEt_2, and fluorescence spectras of (b) CyO-NEt_2, (d) CyS-NEt_2 and (f) CySe-NEt_2 in different solvents including toluene, benzene, DCM, THF, 1,4-dioxane, EtOH, MeOH, MeCN, DMSO, DMF, H_2O and PBS, 10 μM.

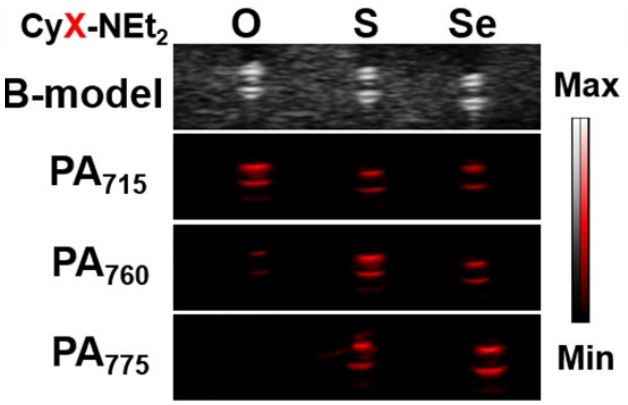

Figure S2. Photograph of the PA signals of CyX-NEt2 (X=O, S, Se).

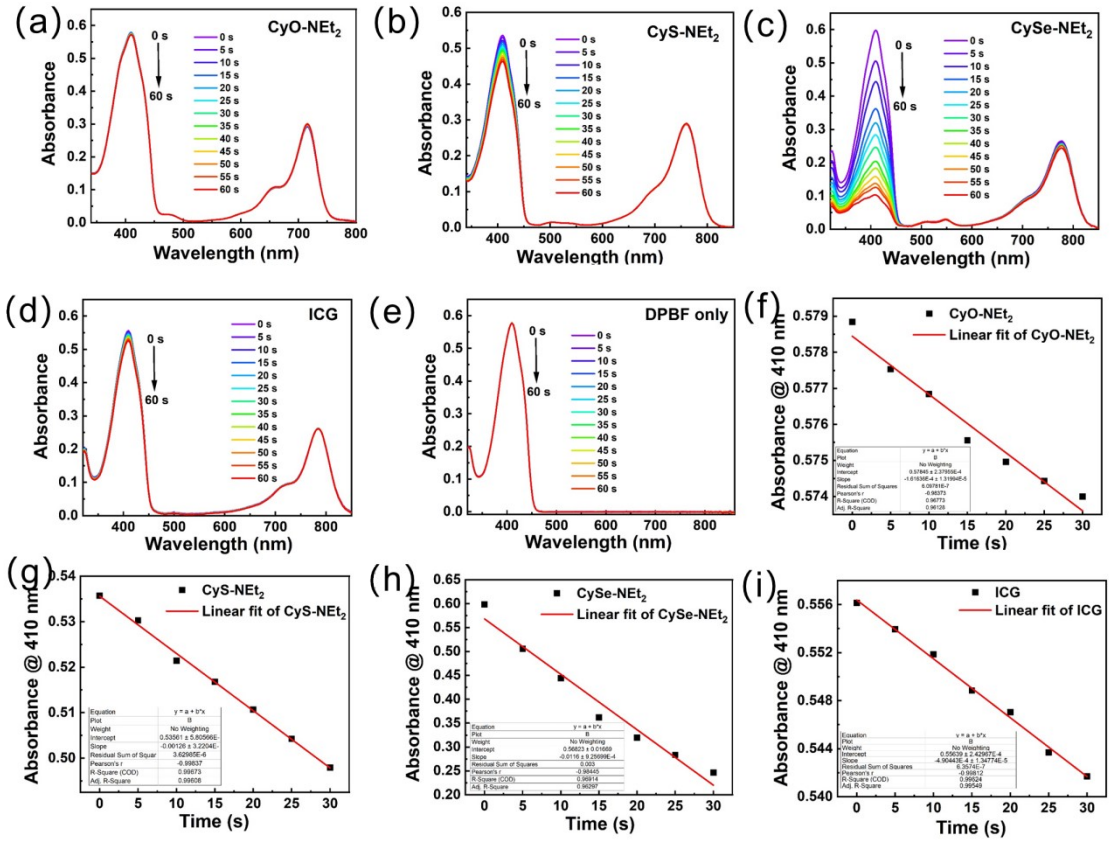

Figure S3. Photodegradation curves of DPBF with (a) CyO-NEt$_2$, (b) CyS-NET$_2$, (c) CySe-NEt$_2$, (d) ICG and (e) DPBF only under 750 nm light irradiation for 60 s, 5 mW/cm^2. Linear fit of absorbance at 410 nm for DPBF degradation with (f) CyO-NEt$_2$, (g) CyS-NEt$_2$, (h) CySe-NEt$_2$ and (i) ICG under 750 nm light irradiation.

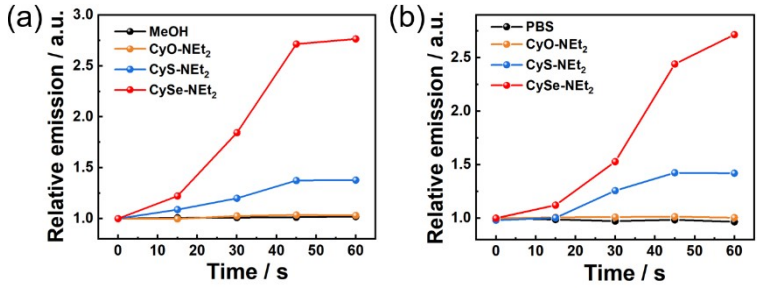

Figure S4. Relative emission enhancement at 530 nm of SOSG with CyX-NEt2 (X=O, S, Se) in (a) methanol (slit = 3) and (b) PBS buffer (slit = 5) under 750 nm light irradiation (5 mW/cm2). λex/em = 480 nm/530 nm

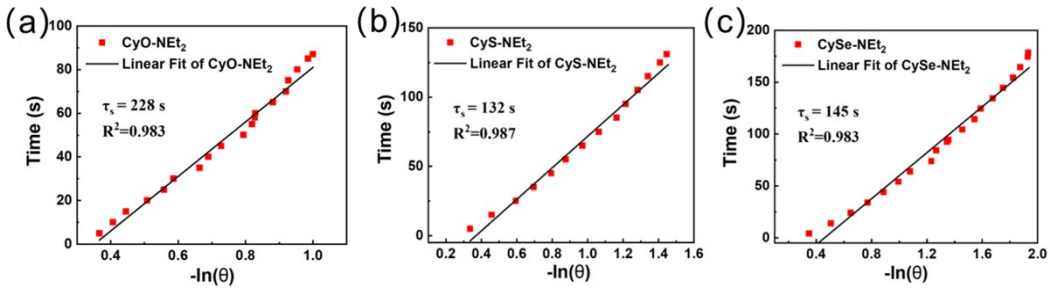

Figure S5. Time constants for calculating photothermal conversion efficiency of CyX-NEt_2 (X=O, S, Se).

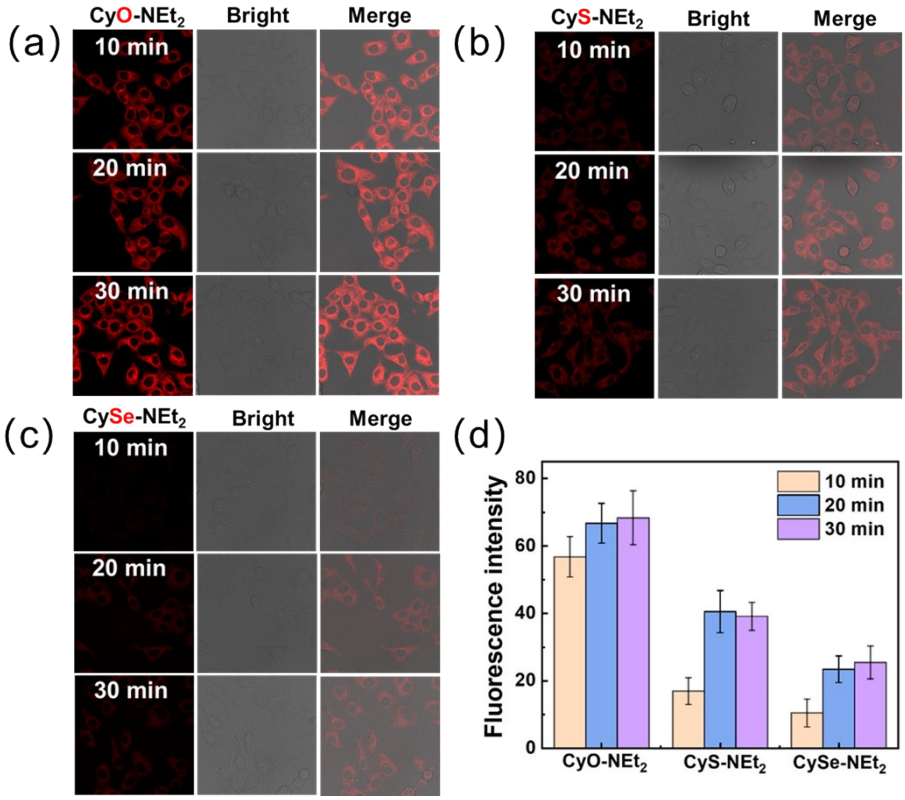

Figure S6. Confocal images of 4T1 cells with 4 μM compound CyX-NEt_2 (X=O, S, Se) at different incubation times. Ex: 670 nm, Em: 680-800 nm.

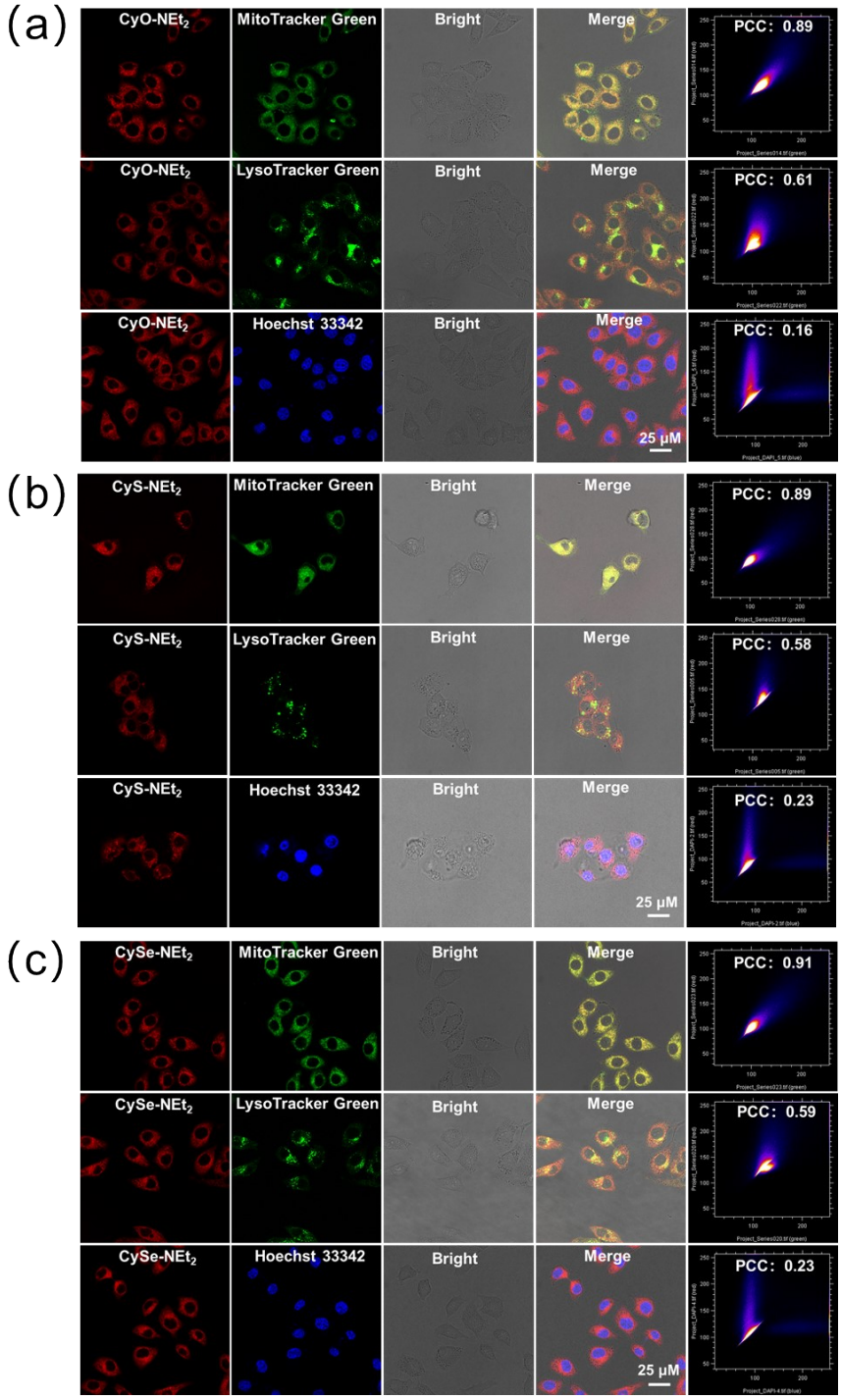

Figure S7. Subcellular colocalization images of 4 μM compound (a) CyO-NEt_2, (b) CyS-NEt_2 and (c) CySe-NEt_2 (Ex: 670 nm, Em: 680-800 nm) in 4T1 cells with MitoTracker Tracker Green, LysoTracker Green, and Hoechst 33342 (1 μM), respectively. The green channel was excited at 488 nm, and collected at 500-550 nm. The blue channel was excited at 405 nm, and collected at 440-480 nm. The scale bar represents 25 μm.

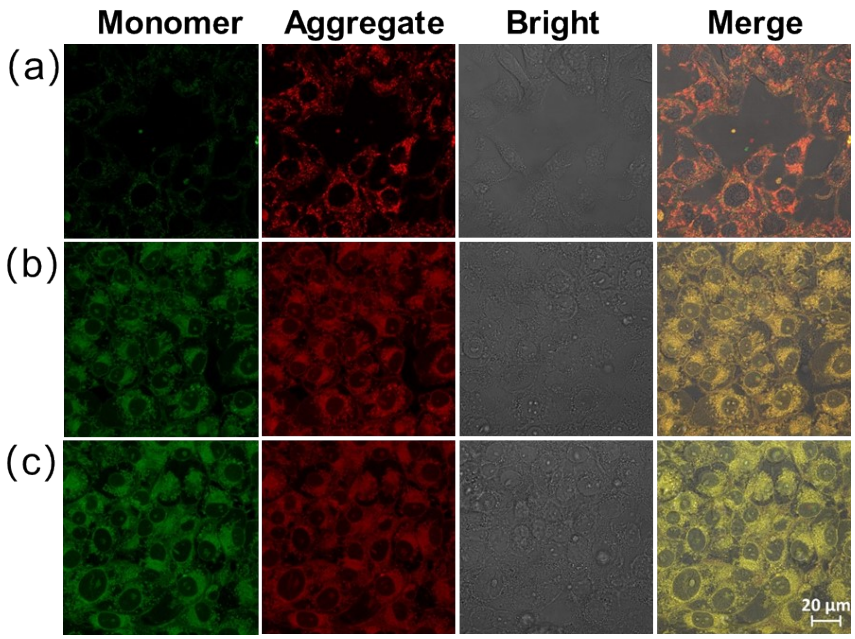

Figure S8. JC-1 assay for the mitochondrial membrane potential decrease for CySe-NEt_2 in Hypoxia. 4T1 cells were incubated with (a) 0 μM, (b) 0.2 μM and (c) 0.4 μM CySe-NEt_2 at 37 °C for 4 h under 750 nm light irradiation; monomer:; aggregate: $\lambda_{ex/em}$ =488/500-550 nm; $\lambda_{ex/em}$ = 514/550-650 nm

Table S1 IC50 values of CyX-NEt_2 against 4T1 cells (24 h).

Compound	Dark[a] [μM]	Light[b] [μM]	PI[c]
CyO-NEt_2	12.08±0.16	> 4	< 3.0
CyS-NEt_2	8.02±0.12	2.17±0.07	3.7
CySe-NEt_2	5.33±0.08	0.26±0.10	20.5

[a]The cells were incubated in darkness for 24h. [b]The cells were incubated irradiated with 750 nm light for 5 min (6.0 J/cm^2). [c]PI (phototoxicity index), the ratio of (IC_{50})Dark / (IC_{50})Light.

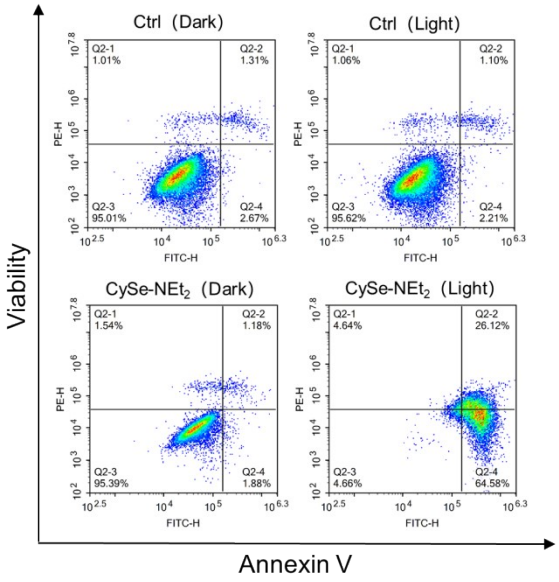

Figure S9. Flow cytometry analysis of 4T1 cells stained with annexin V-FITC/PI after different treatments for compound CySe-NEt_2. dose = 2.0 μM.

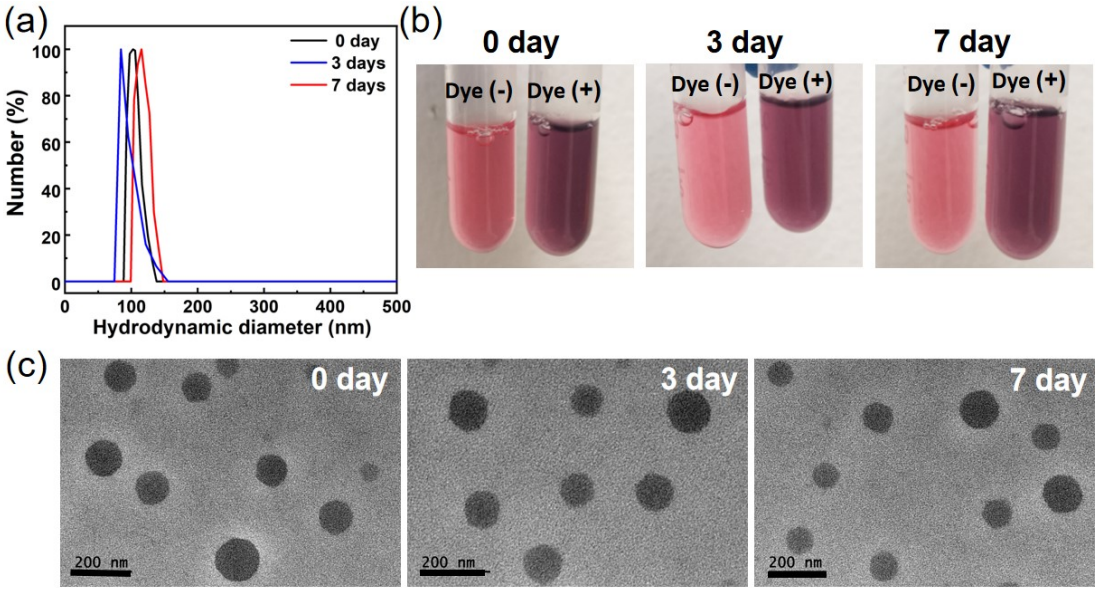

Figure S10. Stability of CySe-mPEG5k. Size distribution of CySe-mPEG5k measured by (a) TEM and (c) DLS for 0 day, 3 day and 7 days respectively, scale bar: 200 nm.

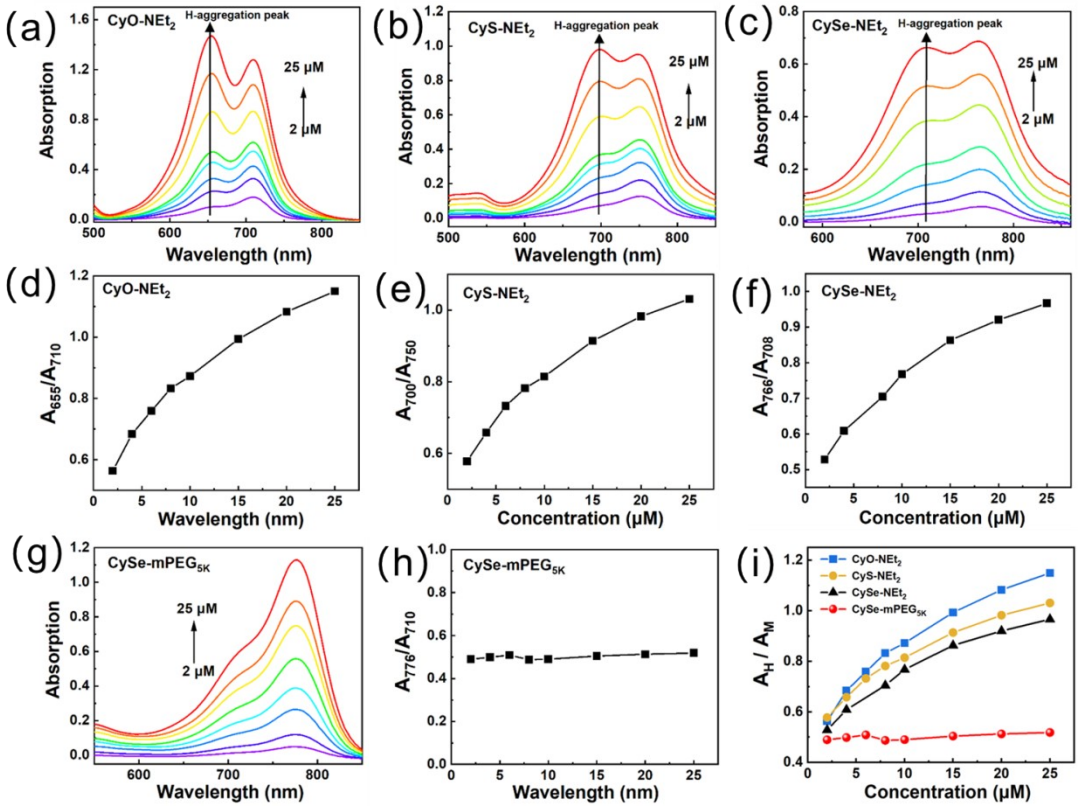

Figure S11. (a-h) Absorption spectras of CyX-NEt_2 (X=O, S, Se) and CySe-$mPEG_{5K}$ at different concentrations in PBS. (i) The corresponding absorbance ratios of A_H/A_M (H-aggregate/Monomer)

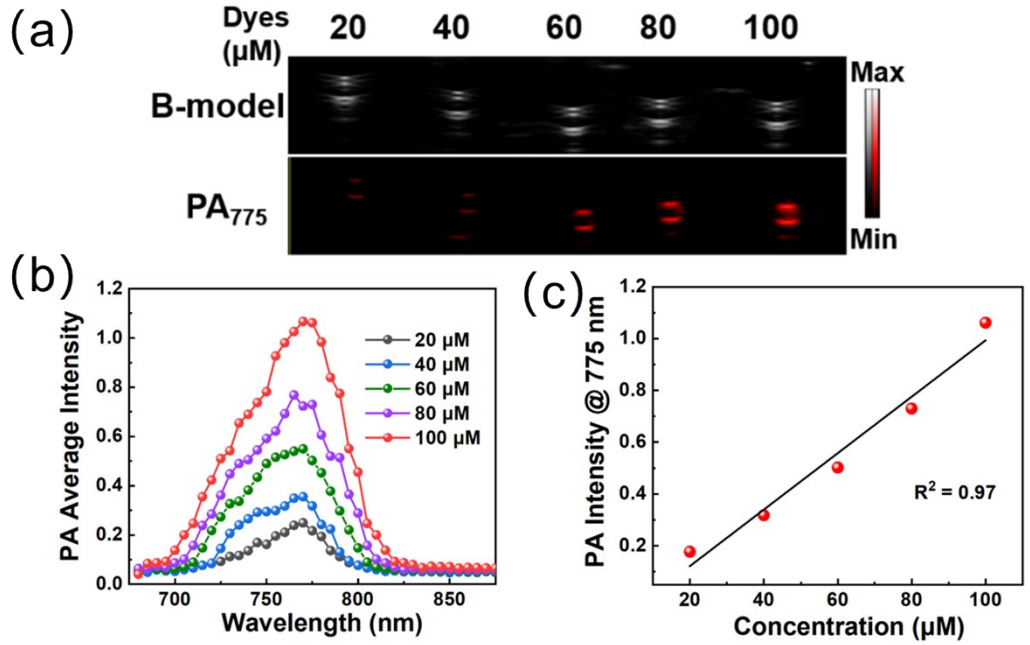

Figure S12. (a) Photograph of the PA signals, (b) photoacoustic spectra of 20~100 μM CySe-mPEG$_{5K}$ (PBS bufffer, pH 7.4) and (c) linear fit of photoacoustic intensities at 775 nm of CySe-mPEG$_{5K}$ at different concentrations in PBS.

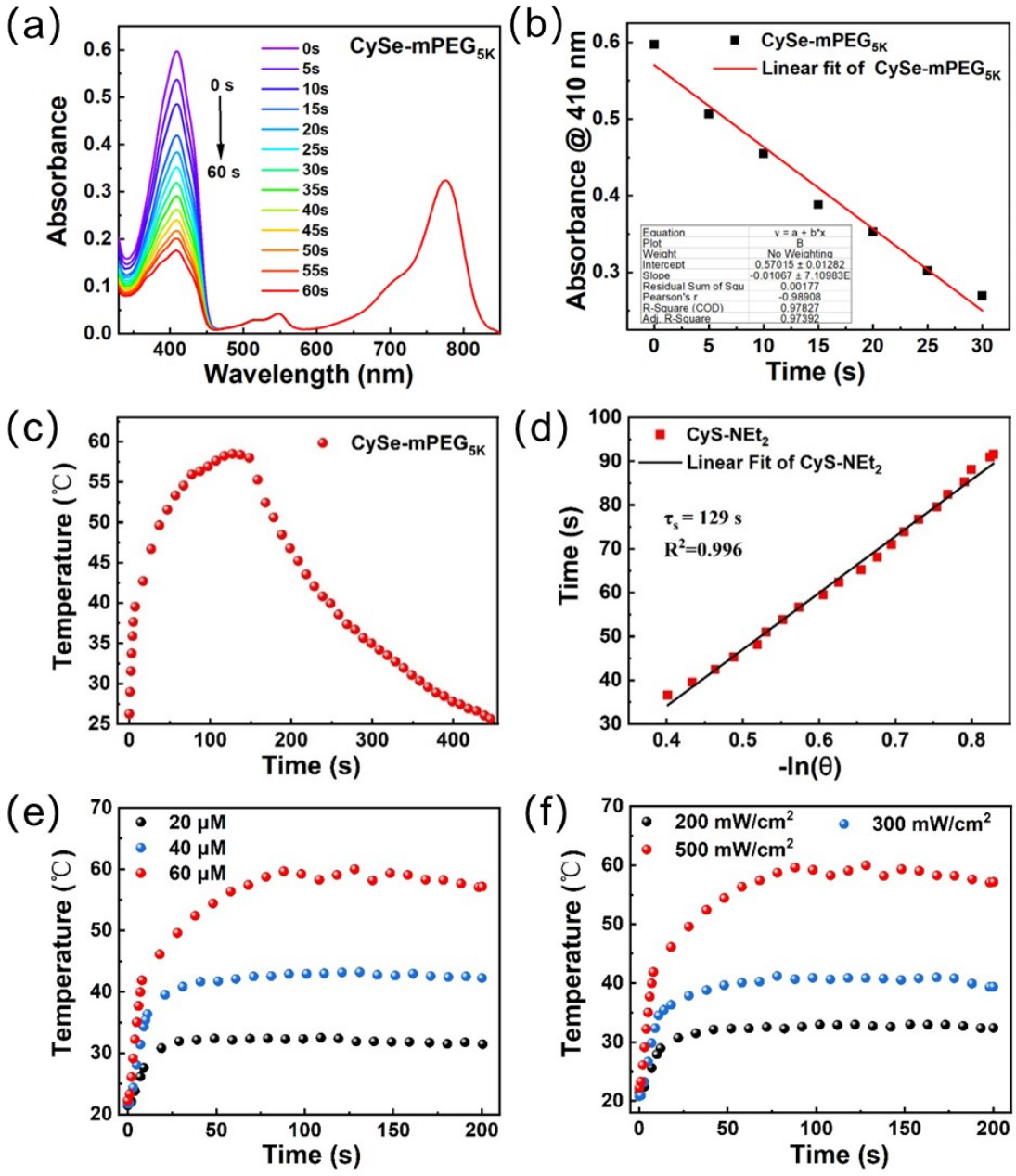

Figure S13. (a) DPBF degradation induced by CySe-mPEG$_{5K}$ and (b) Linear fit of absorbance at 410 nm for DPBF degradation under 750 nm light irradiation, 5.0 mW/cm^2. (c) Photothermal effects observed upon irradiating CySe-mPEG$_{5K}$ with 750 nm laser (0.5 W/cm^2), and then the laser was switched off. (d) Time versus ln(θ) plot (with θ being the driving force temperature) obtained using the data recorded during

the cooling period of the experiment. Temperature rise after 750 laser irradiation for CySe-mPEG$_{5K}$ with different (e) concentrations or (f) laser powers in PBS solution.

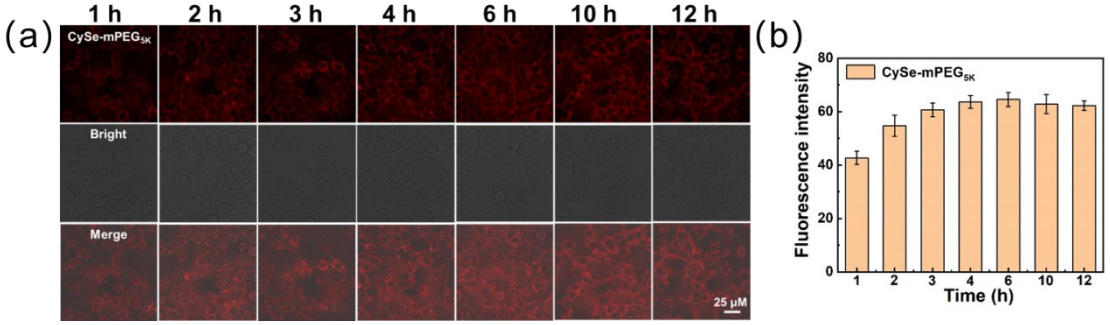

Figure S14. Confocal images of 4T1 cells with 4 μM CySe-mPEG$_{5K}$ at different incubation times. Ex: 670 nm, Em: 680-800 nm. The scale bar represents 25 μm.

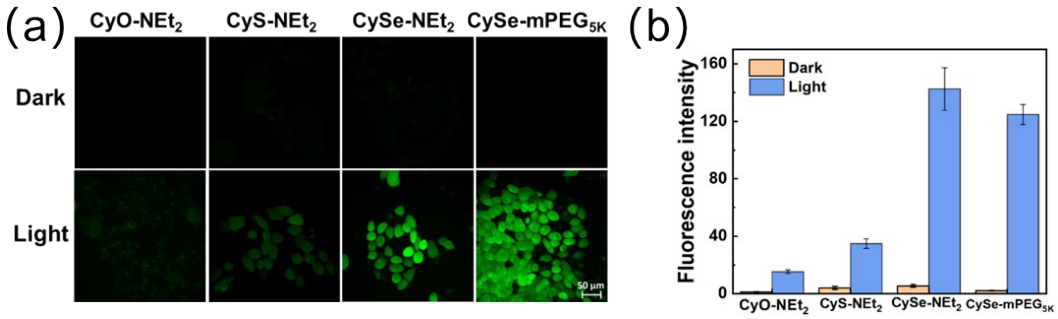

Figure S15. (a) Cellular ROS production in 4T1 cells incubated with 10 μM DCFH-DA and 4 μM CyX-NEt$_2$ (X=O, S or Se) or CySe-mPEG$_{5K}$ under dark and 750 nm light irradiation (20 mW/cm^2, 5 min). (b) Average Fluorescence emission intensities of (b). Ex: 488 nm, Em: 500-550 nm. The scale bar represents 50 μm.

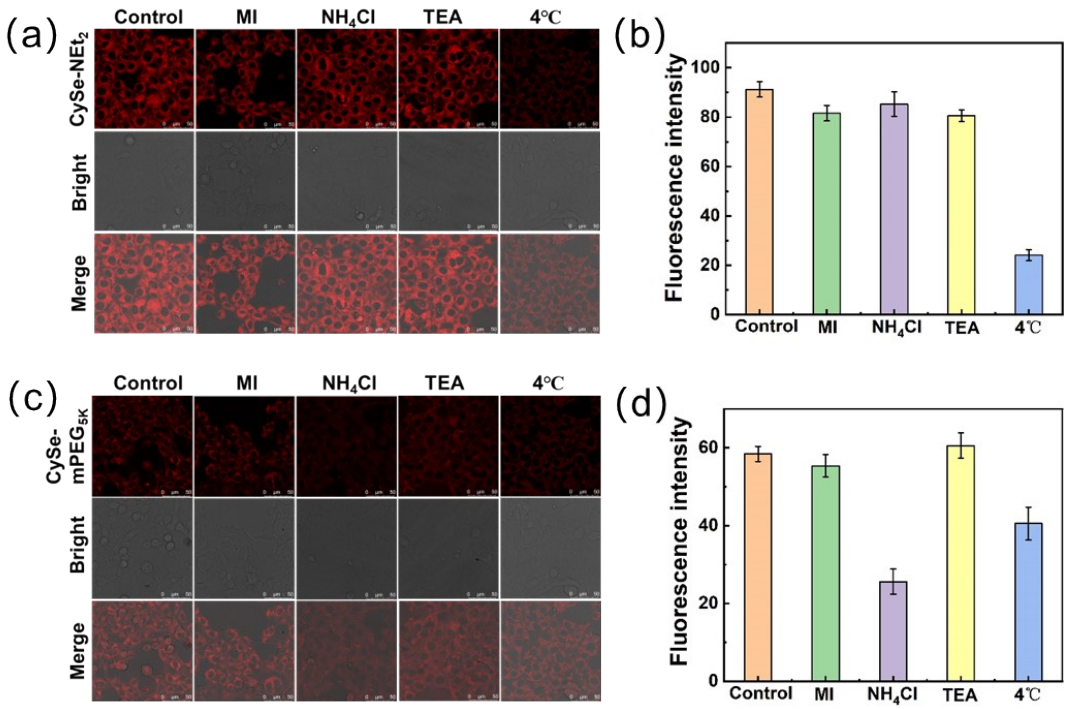

Figure S16. Internalization pathway studies of 4 μM compound (a,b) CySe-NEt_2 and (c,d) CySe-$mPEG_{5K}$. Confocal images and fluorescence intensity of 4T1 cells after incubation with compounds along with different endocytosis inhibitors. Ex: 670 nm, Em: 680-800 nm.

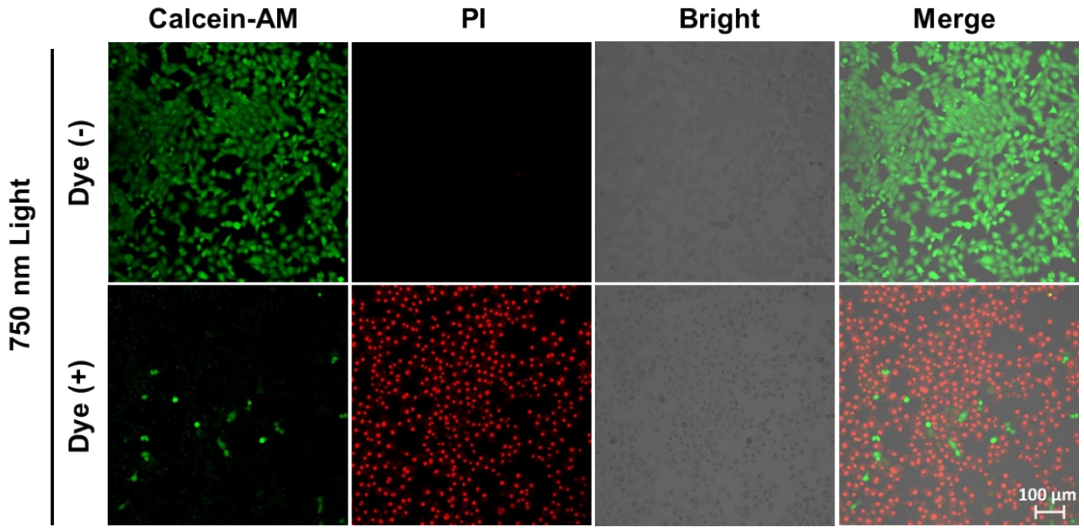

Figure S17. Fluorescence images of 4T1 cells labeled with calcein-AM (green, live cells) and propidium iodide (red, dead cells) in live dead costaining experiments after incubation of CySe-$mPEG_{5K}$ without light or 750 nm laser irradiation (500 mW/cm^2, 3 min). The scale bar represents 100 μm.

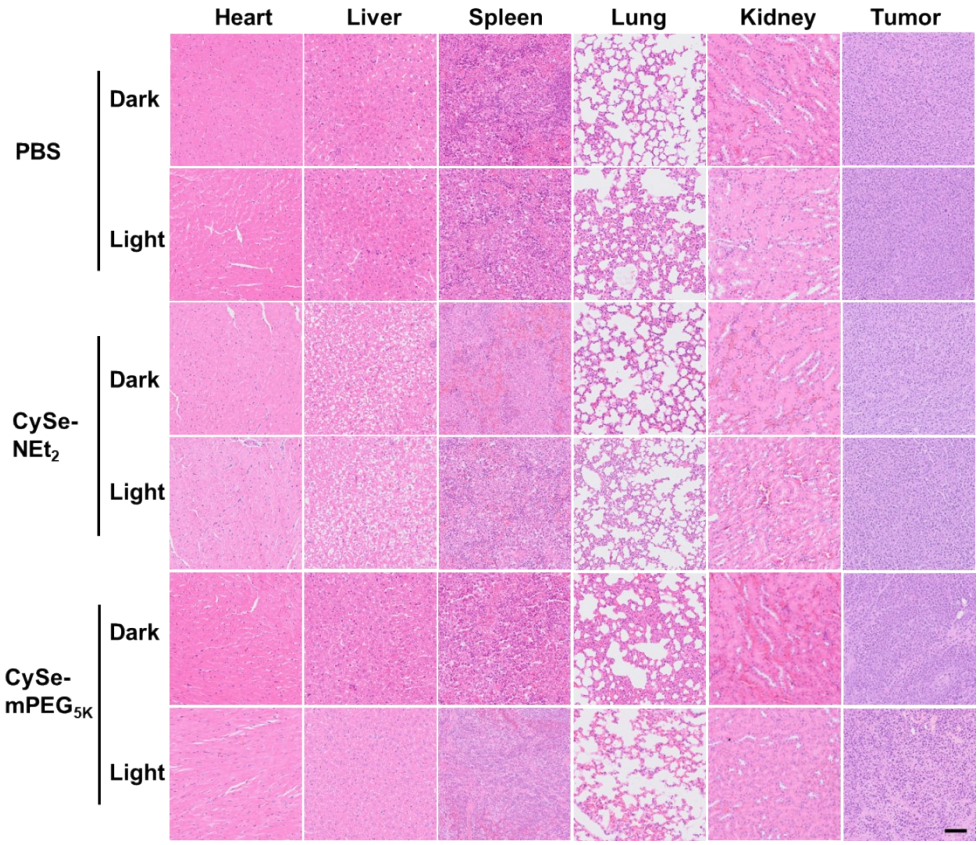

Figure S18. H&E staining analysis of tumor tissue sections from three groups of mice. All the images shared the same scale bar of 100 μm.

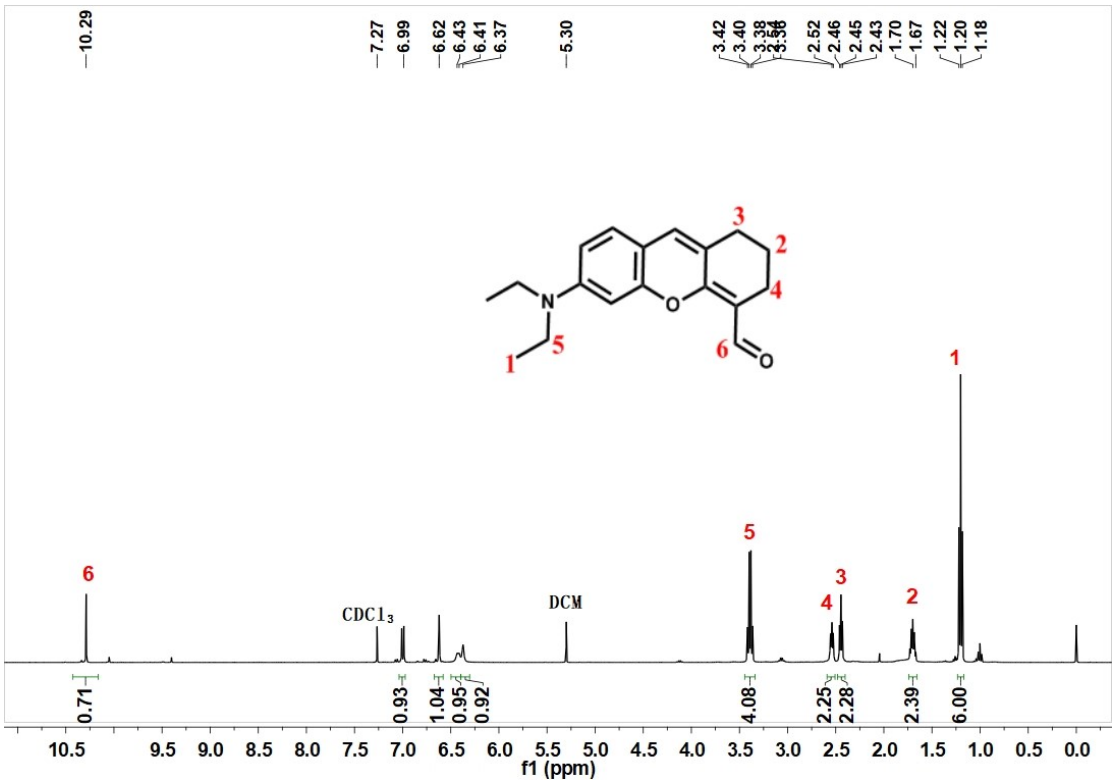

Figure S19. ^{1}H NMR spectrum of CyCHO-NEt$_2$ (400 MHz) in CDCl$_3$

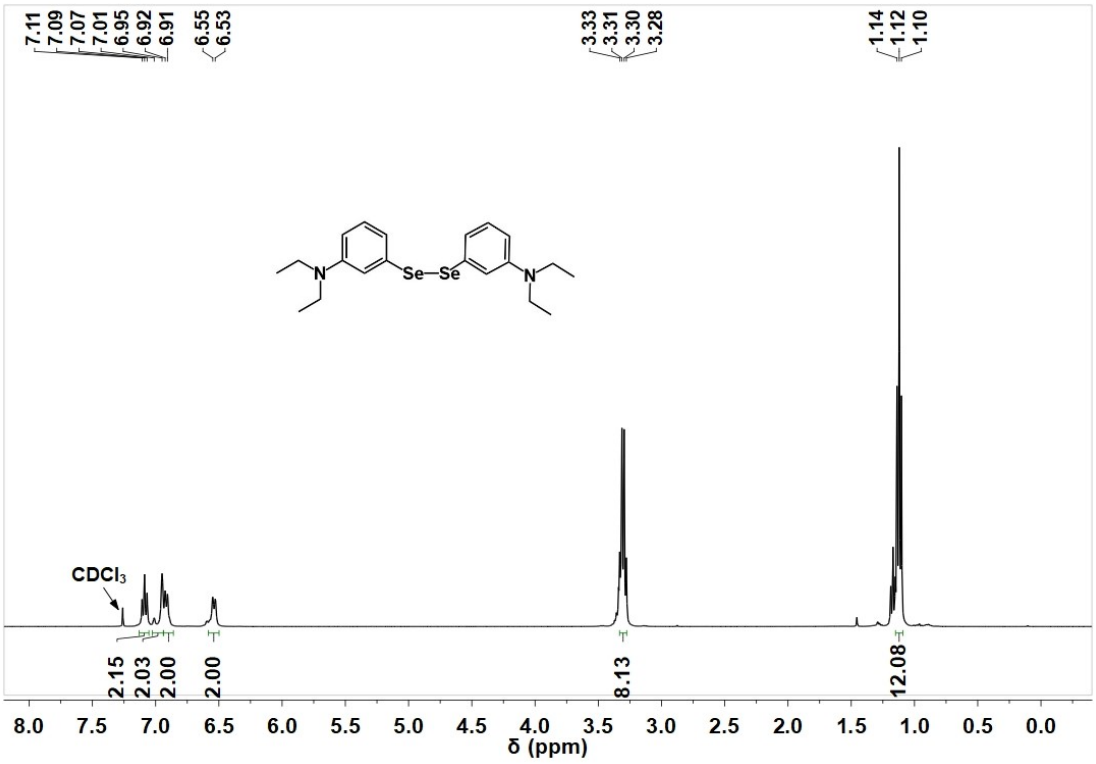

Figure S20. ^{1}H NMR spectrum of 2ArSe-NEt_2 (400 MHz) in $CDCl_3$

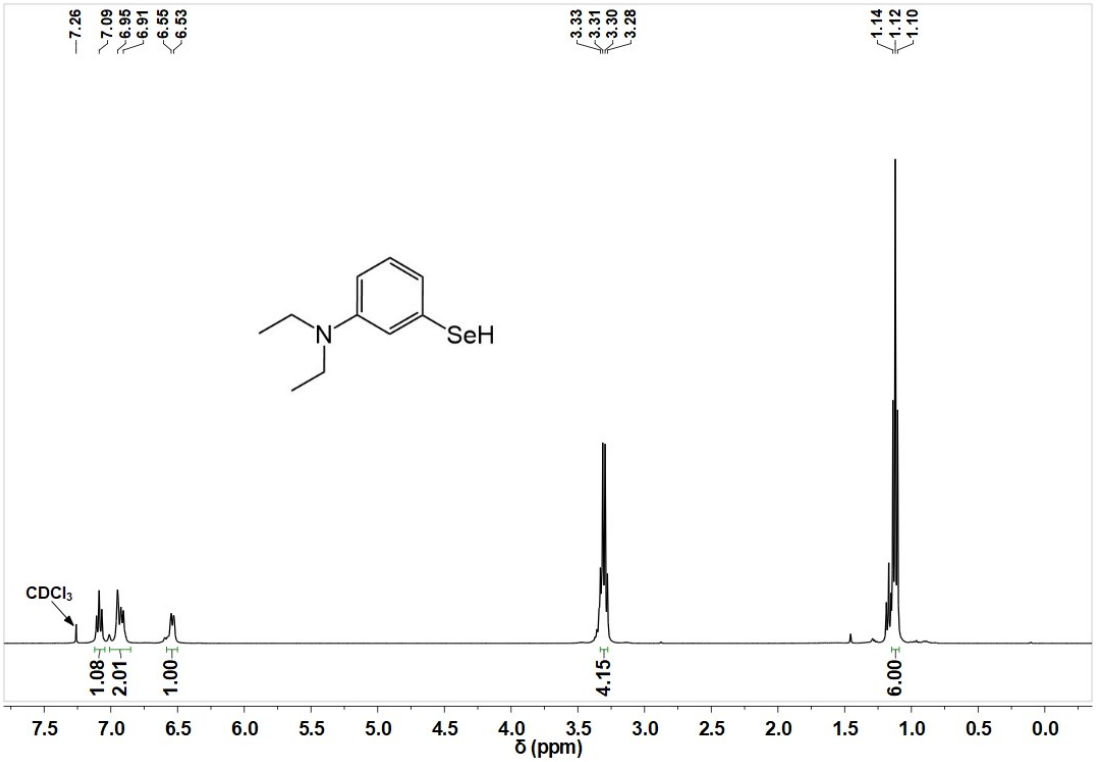

Figure S21. ^{1}H NMR spectrum of ArSeH-NEt_2 (400 MHz) in $CDCl_3$

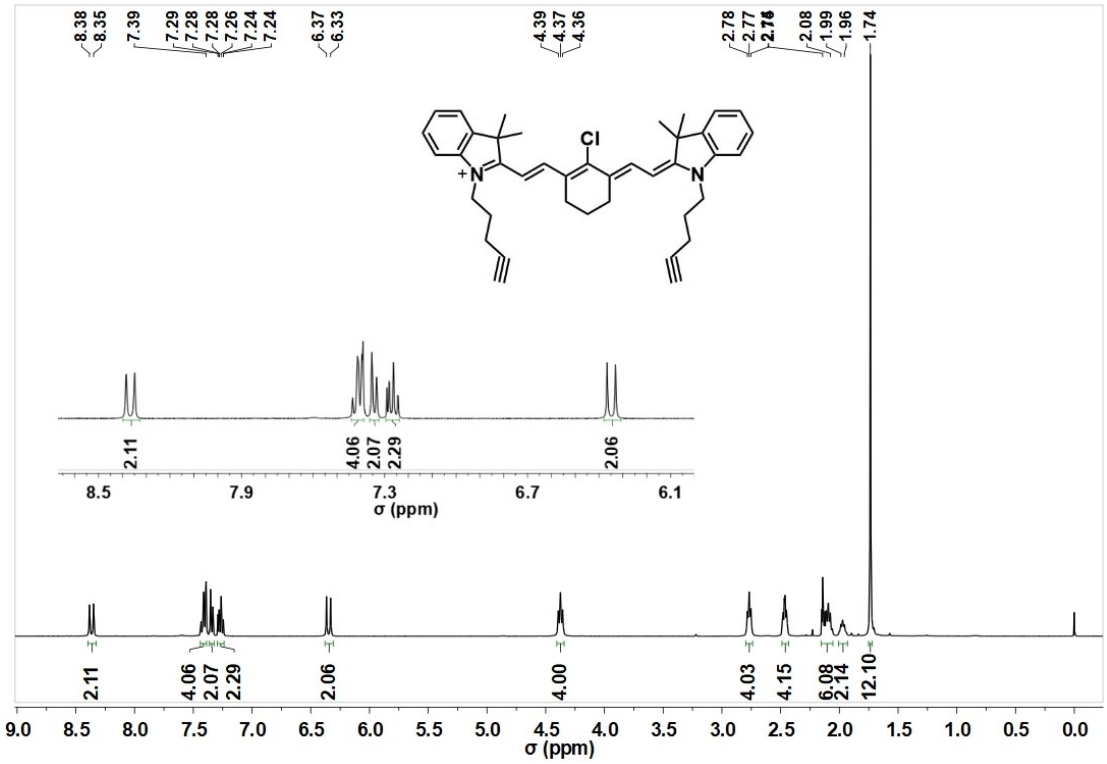

Figure S22. ^{1}H NMR spectrum of IR780-Alkynyl (400 MHz) in $CDCl_3$

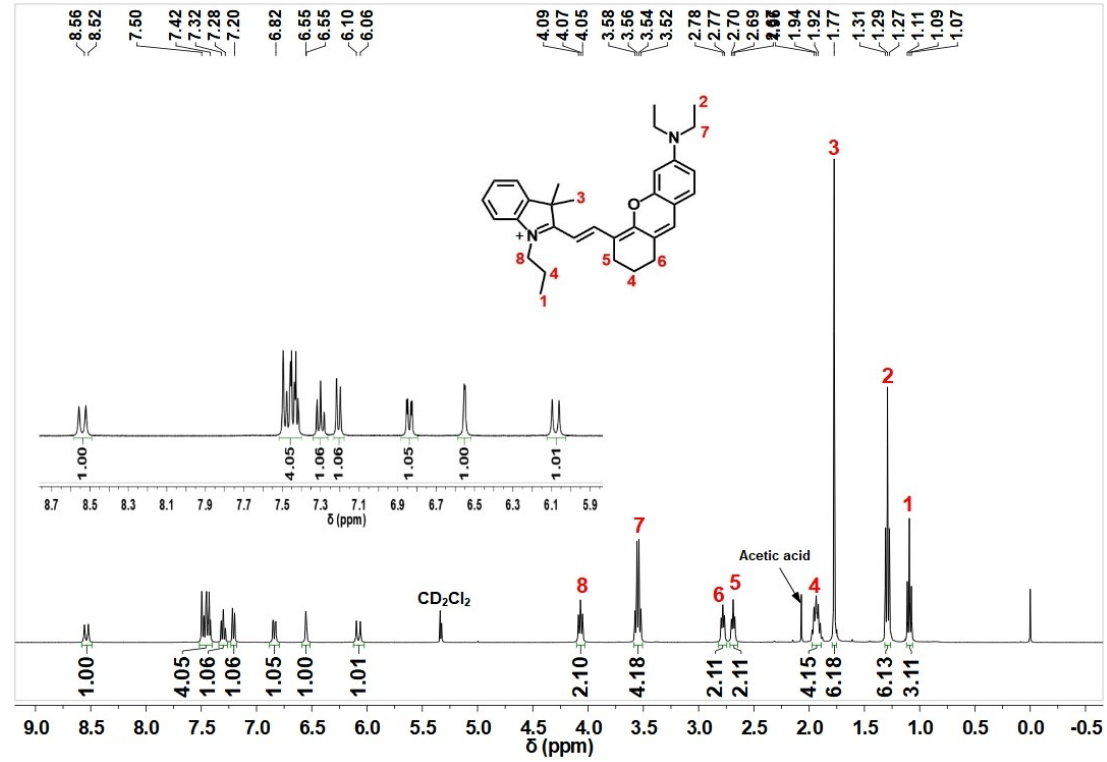

Figure S23. ^{1}H NMR spectrum of CyO-NEt_2 (400 MHz) in CD_2Cl_2

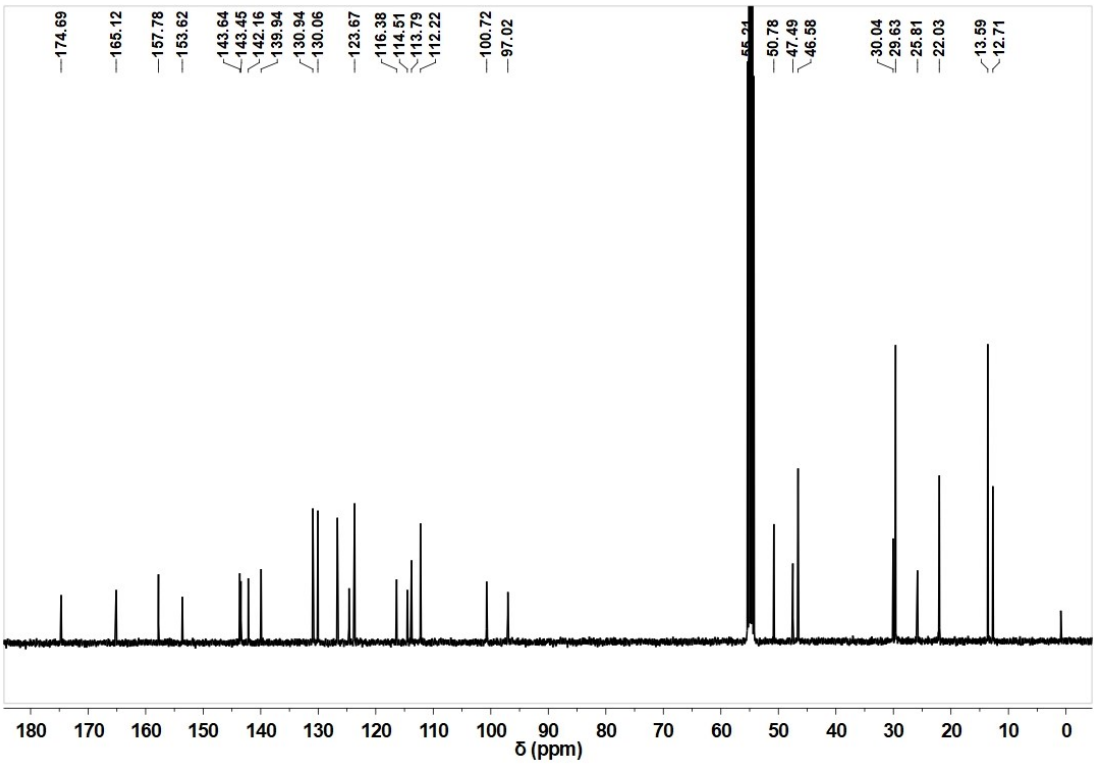

Figure S24. ^{13}C NMR spectrum of CyO-NEt_2 (100 MHz) in CD_2Cl_2

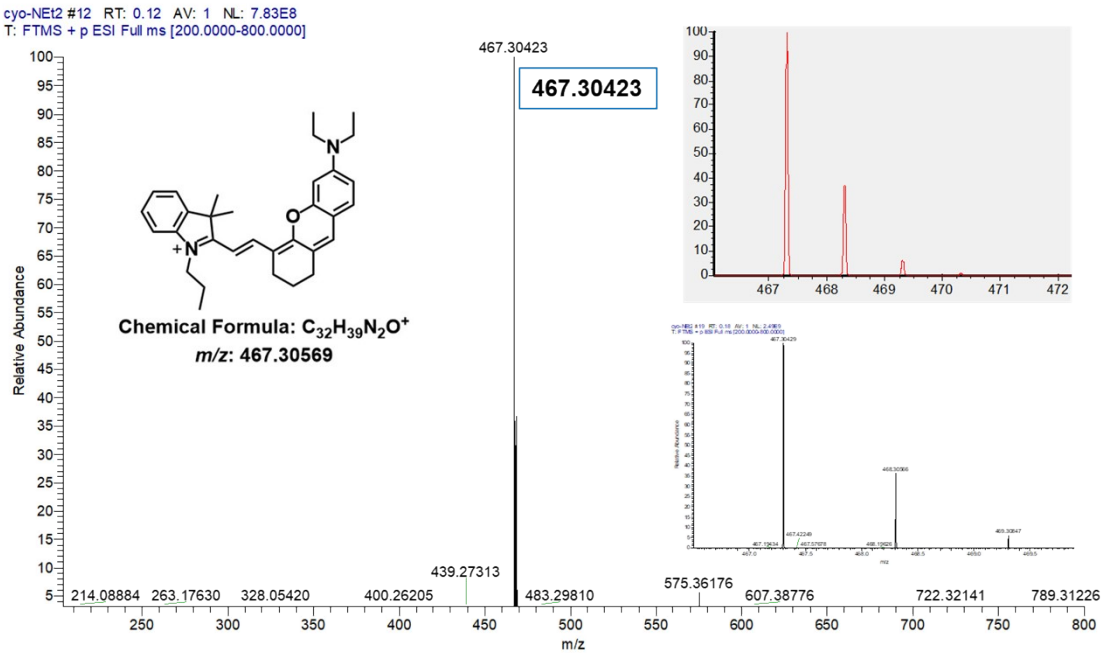

Figure S25. HR-MS spectrum of CyO-NEt_2 (ESI, positive mode)

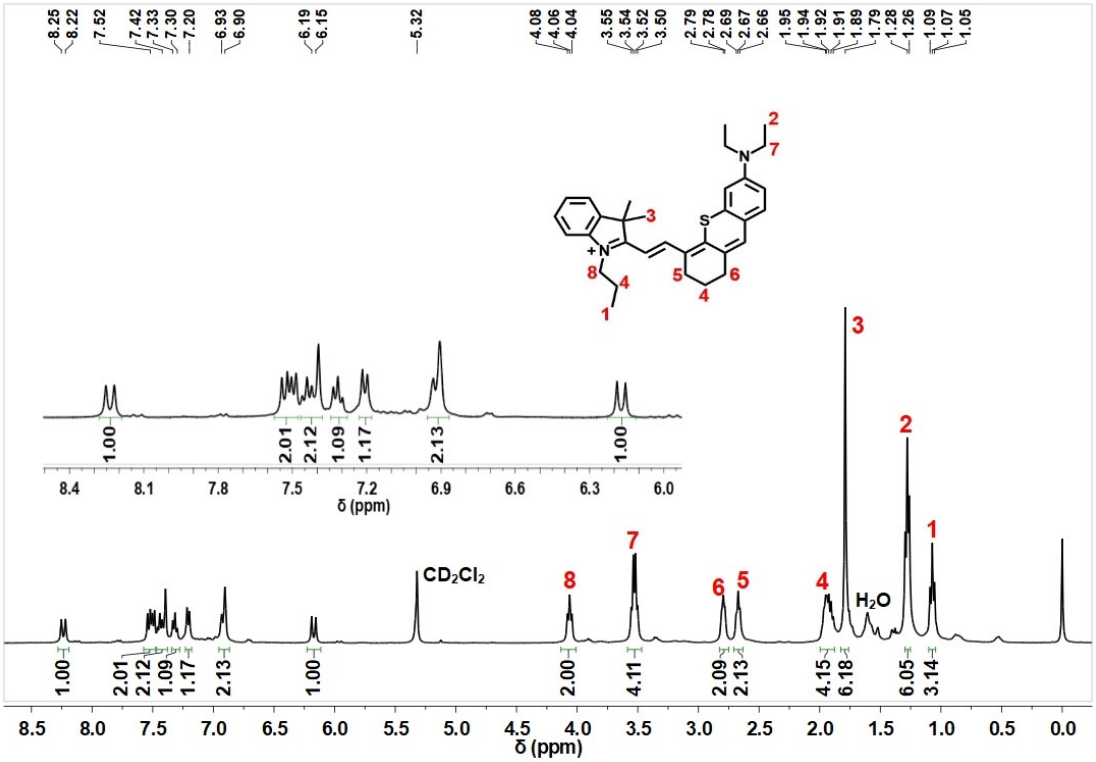

Figure S26. ^{1}H NMR spectrum of CyS-NEt_2 (400 MHz) in CD_2Cl_2

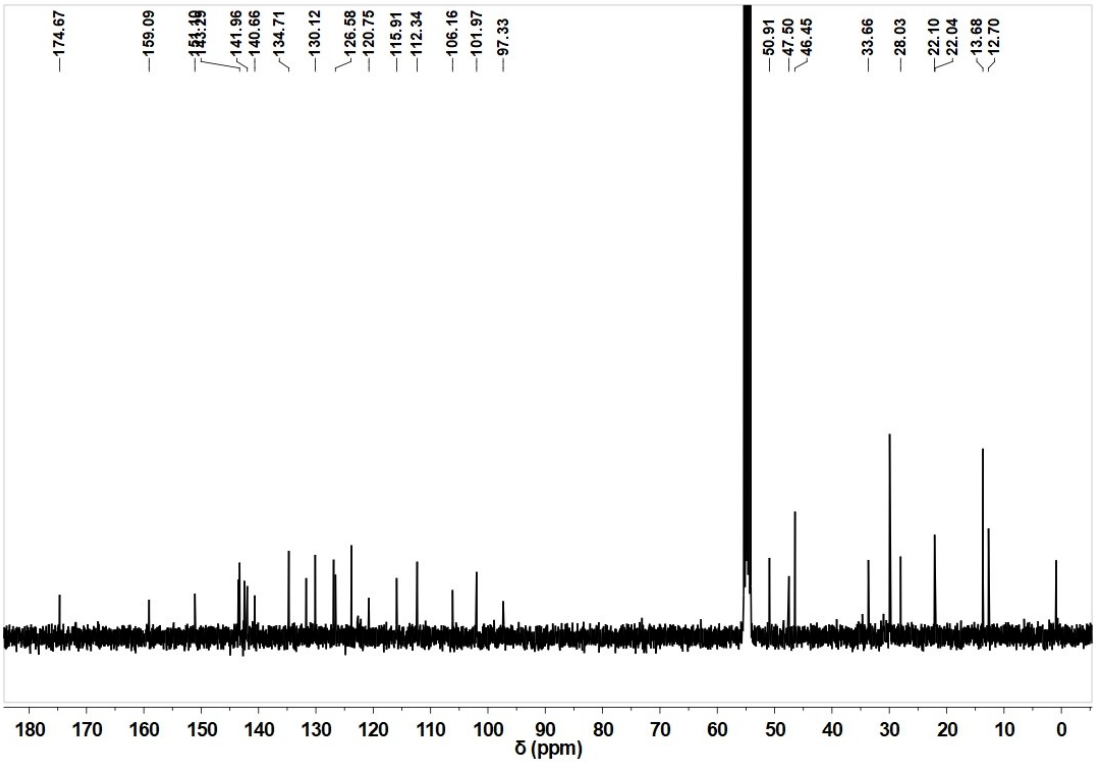

Figure S27. ^{13}C NMR spectrum of CyS-NEt_2 (100 MHz) in CD_2Cl_2

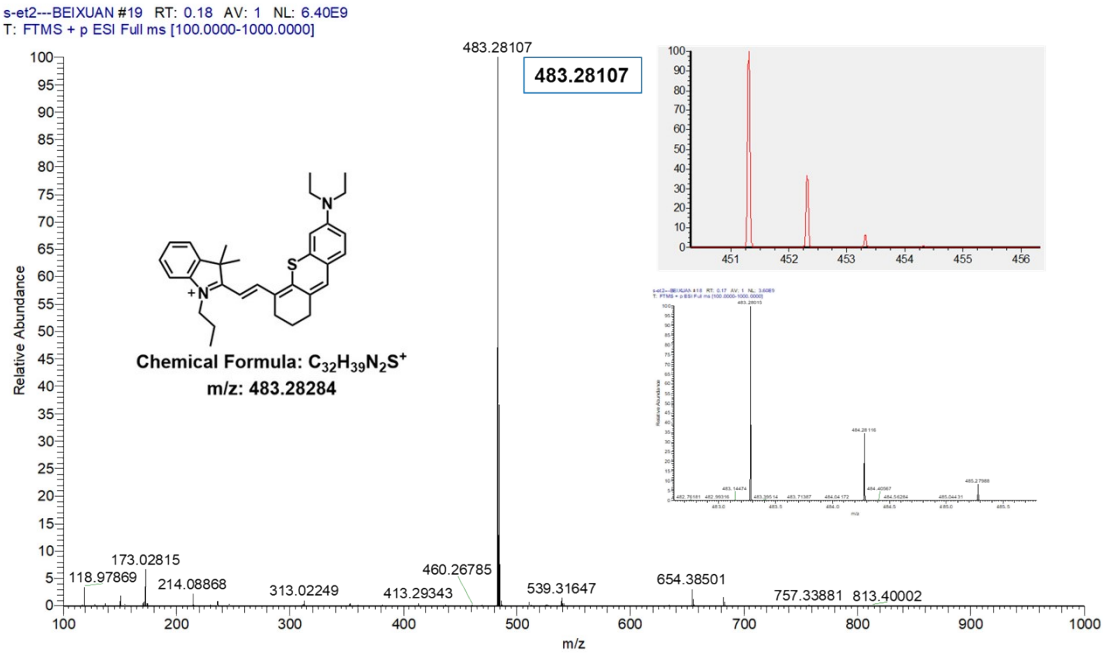

Figure S28. HR-MS spectrum of CyS-NEt_2 (ESI, positive mode)

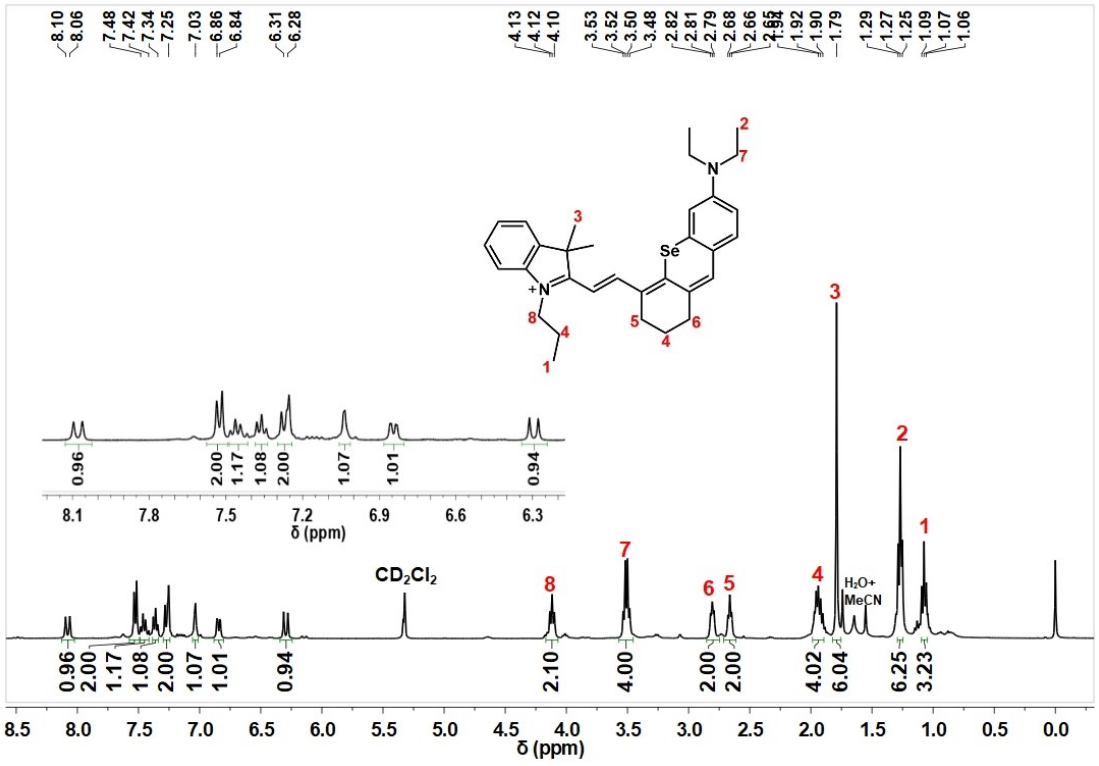

Figure S29. ^{1}H NMR spectrum of CySe-NEt_2 (400 MHz) in CD_2Cl_2

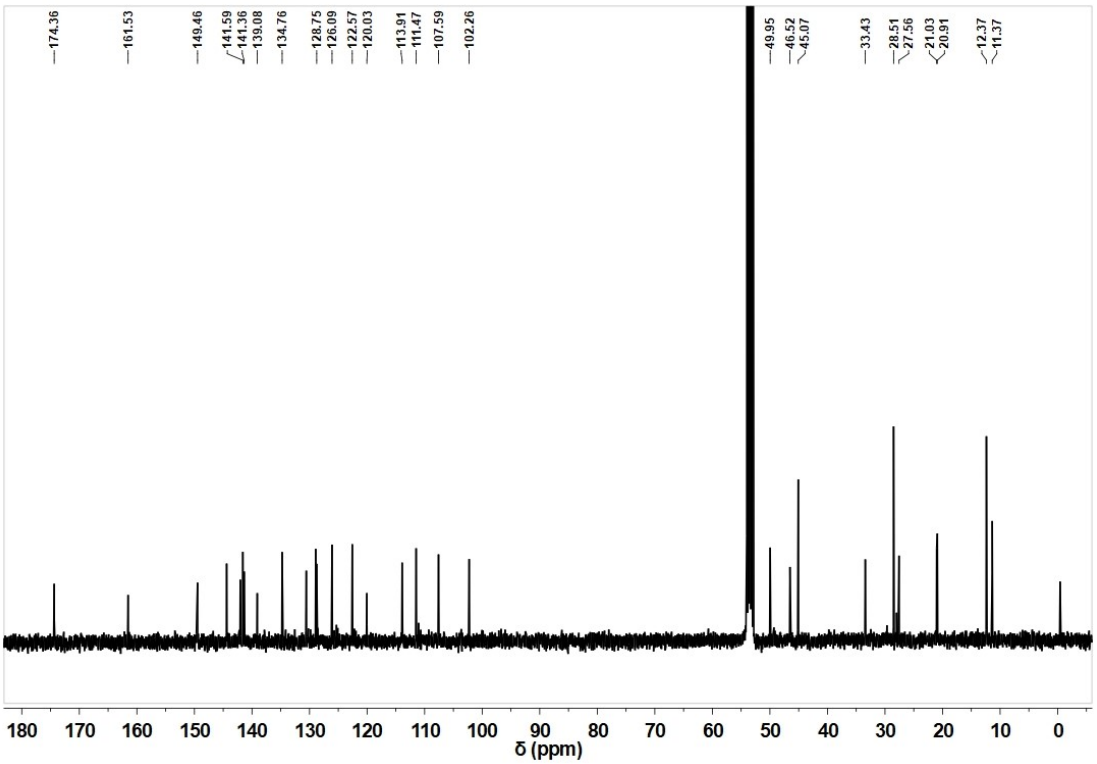

Figure S30. ^{13}C NMR spectrum of CySe-NEt_2 (100 MHz) in CD_2Cl_2

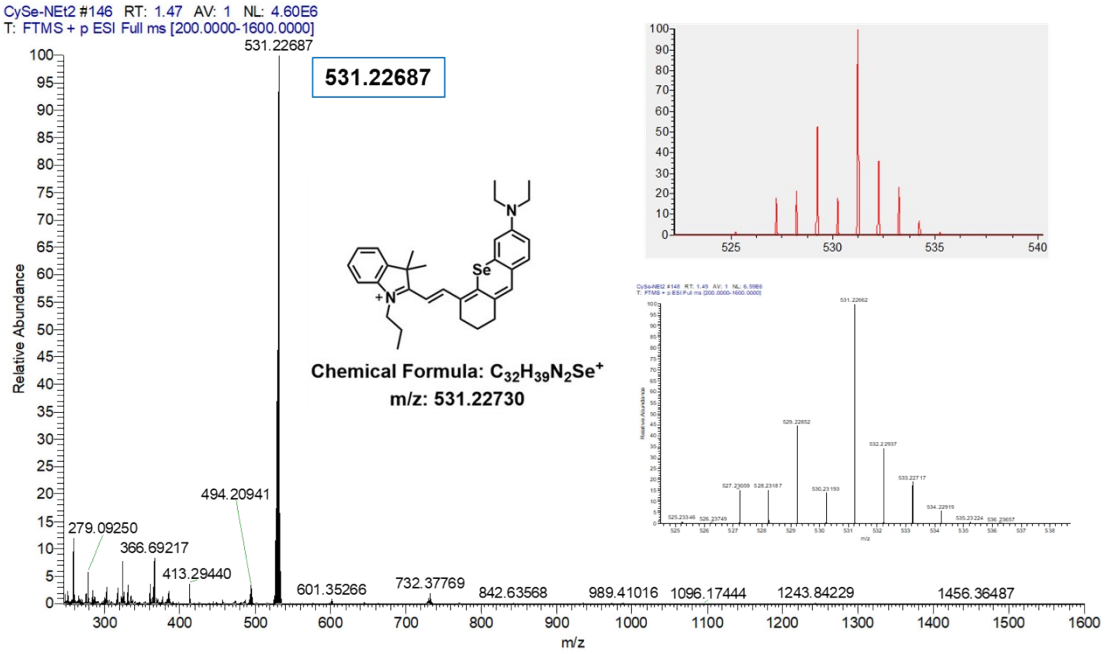

Figure S31. HR-MS spectrum of CySe-NEt_2 (ESI, positive mode)

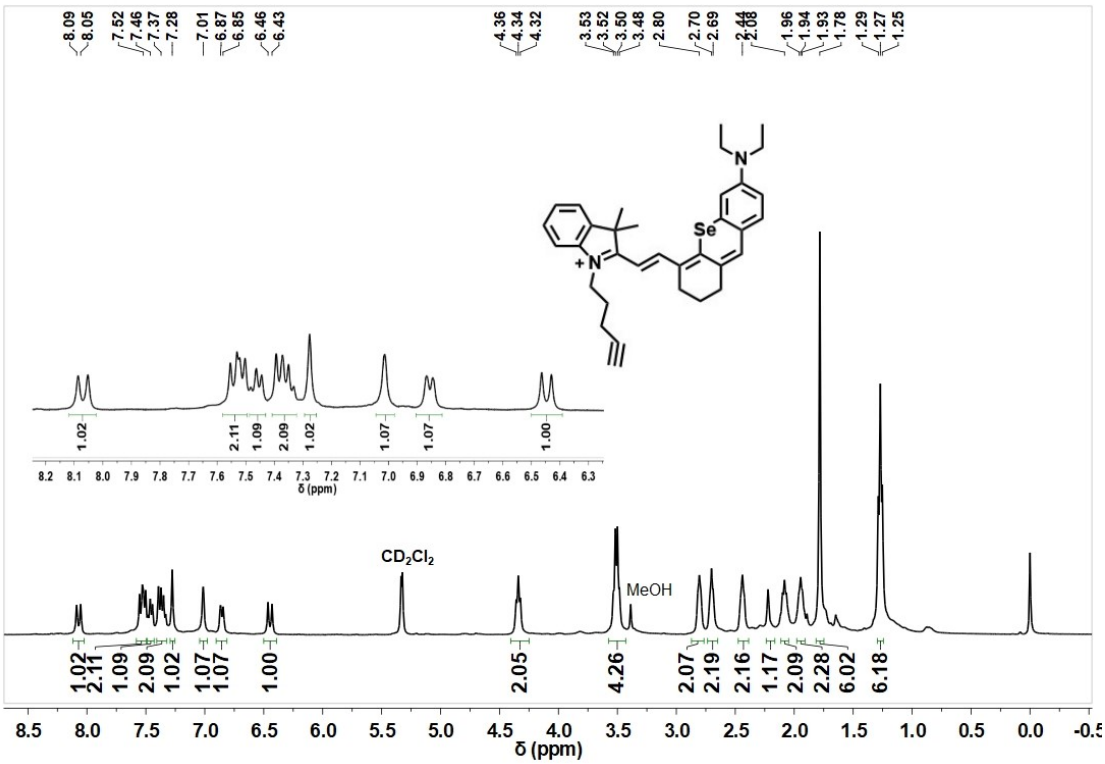

Figure S32. ^{1}H NMR spectrum of CySe-Alkynyl (400 MHz) in CD_2Cl_2

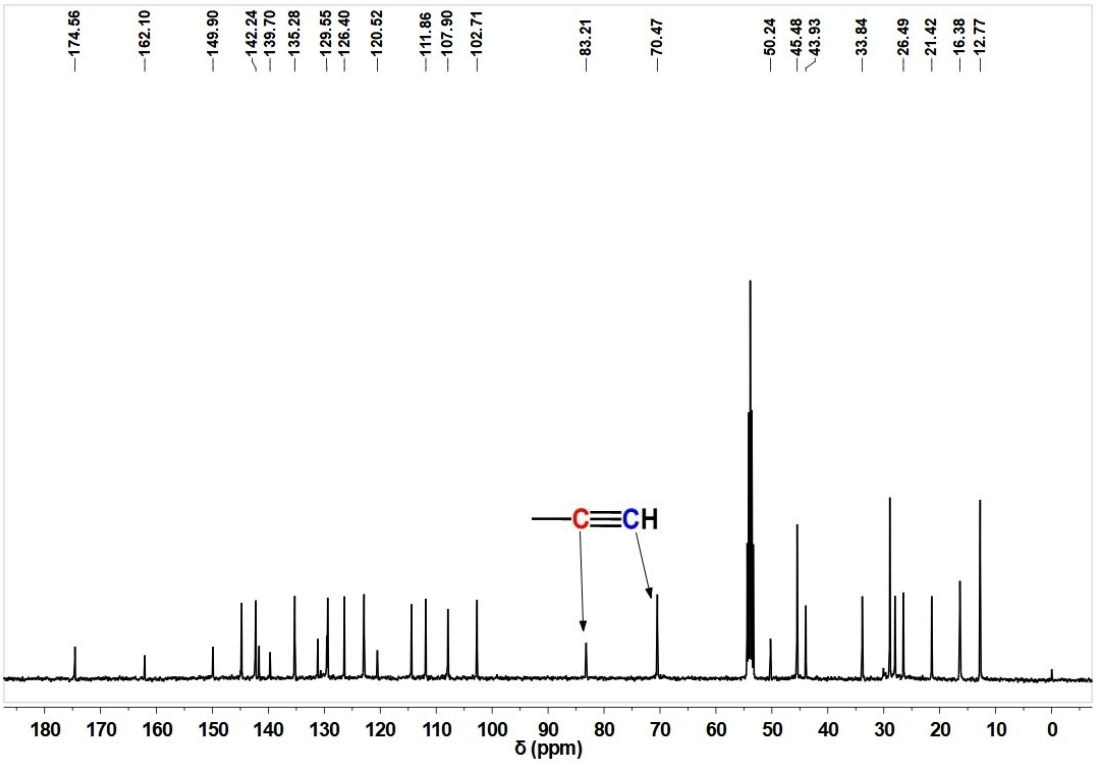

Figure S33. ^{13}C NMR spectrum of CySe-Alkynyl (100 MHz) in CD_2Cl_2.

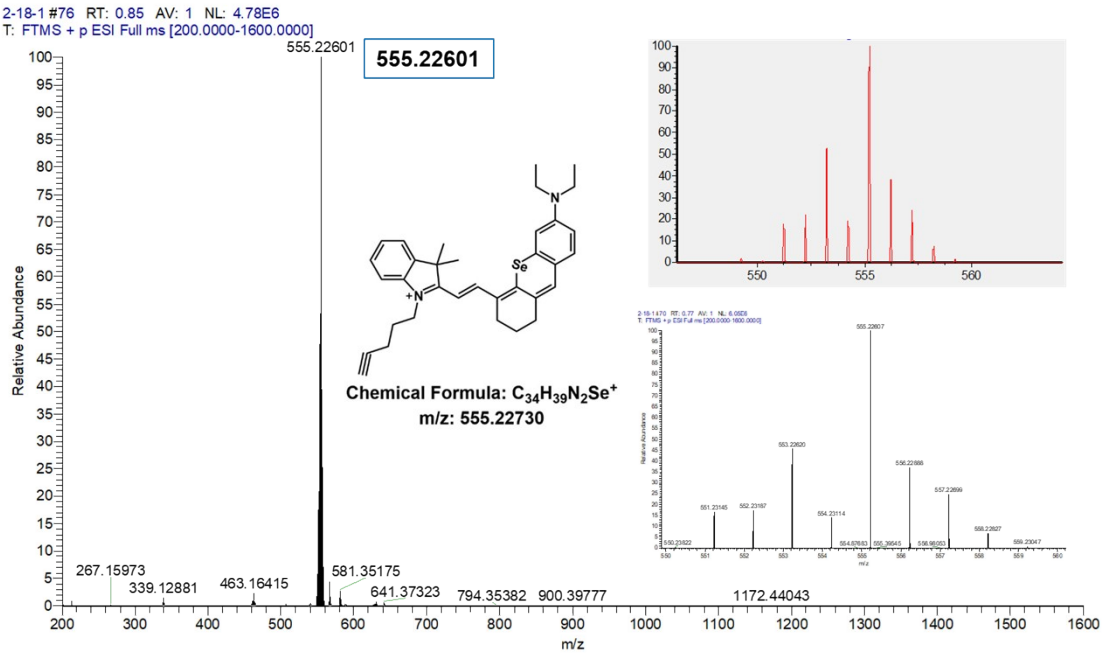

Figure S34. HR-MS spectrum of CySe-Alkynyl (ESI, positive mode).

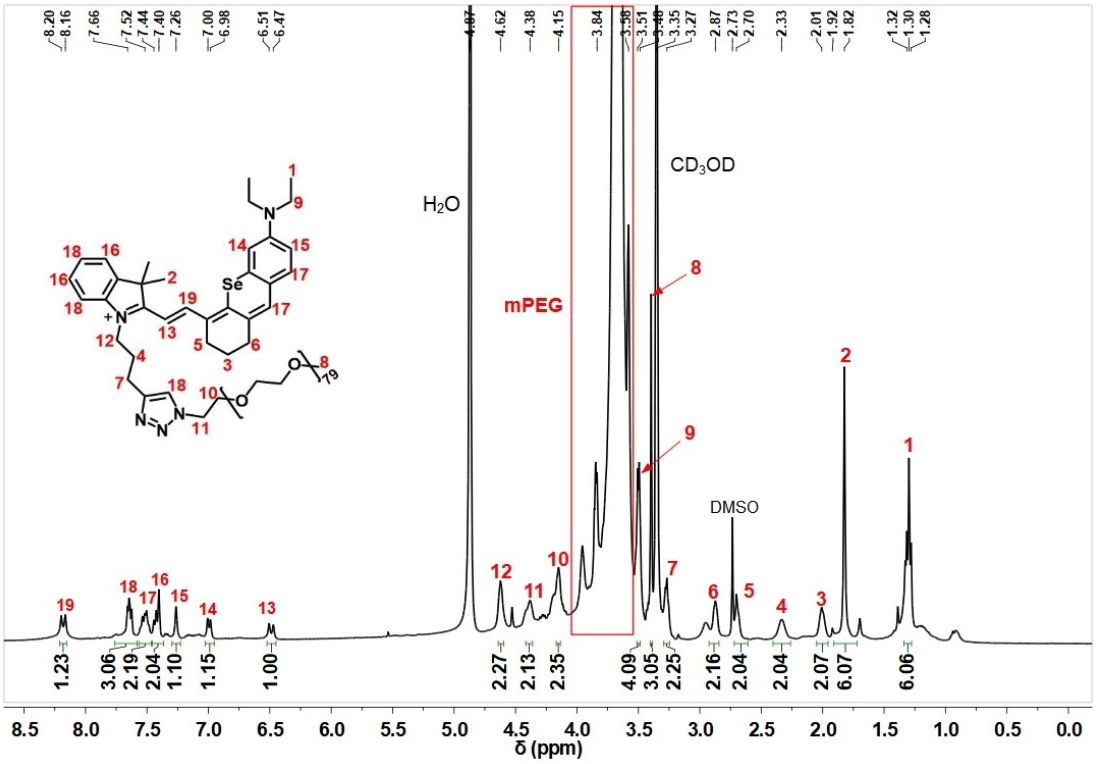

Figure S35. ^{1}H NMR spectrum of CySe-mPEG$_{5K}$ (100 MHz) in methanol-d4.

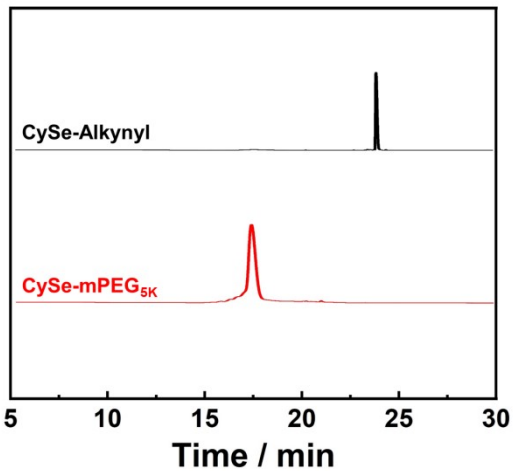

Figure S36. HPLC spectrum of CySe-Alkynyl and CySe-mPEG$_{5K}$.

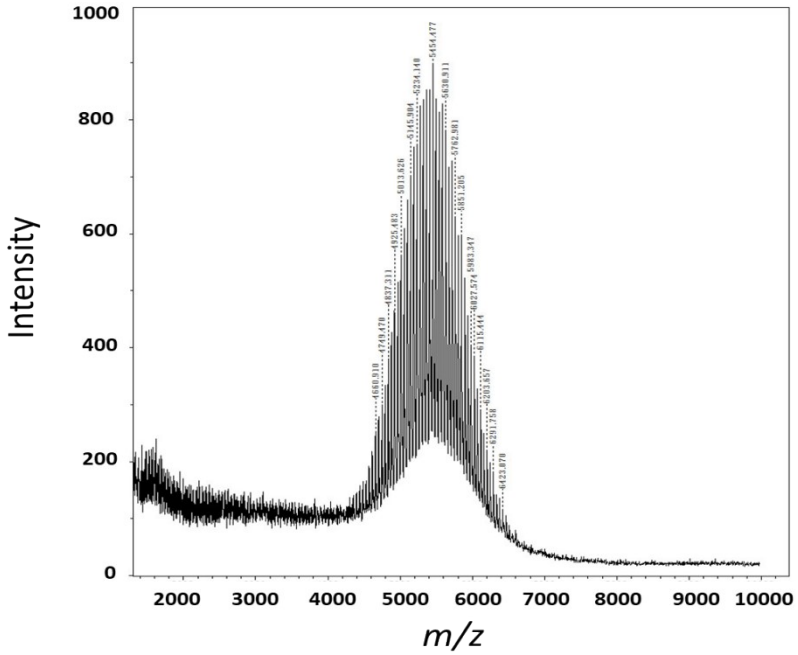

Figure S37. MS spectrum of CySe-mPEG$_{5K}$ (Modi-TOF)

Table S2. Calculated electronic transition energies and ΔE_{SnTm} and spin-orbit coupling (SOC) constants between singlet and triplet states of CyX-NEt_2 (X=O, S, Se).

Energy (eV)	CyO-NET_2	CyS-NEt_2	CySe-NEt_2	$\langle S_n \vert H_{SO} \vert T_m \rangle$ (cm^{-1})	CyO-NET_2	CyS-NEt_2	CySe-NEt_2
S_1	2.14	2.00	1.97	$S_1 \leftrightarrow T_1$	0.04	0.90	5.76
T_1	1.21	1.10	1.08	$S_1 \leftrightarrow T_2$	0.10	1.18	8.13
T_2	2.02	1.83	1.78	$S_1 \leftrightarrow T_3$	0.07	0.92	7.03
T_3	2.69	2.60	2.53	$S_1 \leftrightarrow T_4$	0.17	1.89	11.99
T_4	2.85	2.69	2.68				
ΔE_{S1T1}	0.93	0.90	0.89				
ΔE_{S1T2}	0.12	0.17	0.19				
ΔE_{S1T3}	-0.55	-0.60	-0.56				
ΔE_{S1T4}	-0.71	-0.69	-0.71				

Table S3. The values of $[\langle S_n \vert H_{SO} \vert T_m \rangle / \Delta E_{SnTm}]^2$ for the ISC between singlet and triplet states of CyX-NEt_2 (X=O, S, Se).

$[\langle S_n \vert H_{SO} \vert T_m \rangle / \Delta E_{SnTm}]^2$ ($\times 10^6$)	CyO-NEt_2	CyS-NEt_2	CySe-NEt_2
$S_1 \leftrightarrow T_1$	0.00	0.02	0.65
$S_1 \leftrightarrow T_2$	0.01	0.74	28.26
$S_1 \leftrightarrow T_3$	0.00	0.04	2.43
$S_1 \leftrightarrow T_4$	0.10	0.12	4.40
Sum	0.11	0.92	35.74

The values of R = $[\langle S_n \vert H_{SO} \vert T_m \rangle / \Delta E_{SnTm}]^2$ are unitless.

CyO-NEt_2:

Excitation energies and oscillator strengths:

Excited State 1: Singlet-A 2.1377 eV 579.98 nm f=1.1154
<S**2>=0.000
126 ->127 0.70533
This state for optimization and/or second-order correction.
Total Energy, E(TD-HF/TD-KS) = -1427.41303523
Copying the excited state density for this state as the 1-particle RhoCI density.

Excited State 2: Singlet-A 2.8342 eV 437.45 nm f=0.1763
<S**2>=0.000
125 ->127 0.68529
126 ->128 -0.12876

Excited State 3: Singlet-A 3.5392 eV 350.31 nm f=0.0559
<S**2>=0.000
122 ->127 -0.20424
124 ->127 0.59892
126 ->128 -0.29414

Excited State 4: Singlet-A 3.6445 eV 340.19 nm f=0.2954
<S**2>=0.000
122 ->127 0.16423
123 ->127 -0.16322
124 ->127 0.32582
126 ->128 0.56187

the weight of the individual excitations are printed if larger than 0.01

STATE 1: E= 0.044485 au 1.210 eV 9763.3 cm**-1
124a -> 126a: 0.011713
125a -> 126a: 0.967809

STATE 2: E= 0.074144 au 2.018 eV 16272.6 cm**-1
120a -> 126a: 0.013509
124a -> 126a: 0.920669
125a -> 126a: 0.011421
125a -> 127a: 0.034224

STATE 3: E= 0.098775 au 2.688 eV 21678.6 cm**-1

121a -> 126a: 0.011978
121a -> 127a: 0.010974
123a -> 126a: 0.024816
123a -> 127a: 0.013810
124a -> 126a: 0.028250
124a -> 130a: 0.010068
125a -> 127a: 0.844421

STATE 4: E= 0.104798 au 2.852 eV 23000.4 cm**-1
119a -> 126a: 0.011948
122a -> 128a: 0.010408
123a -> 126a: 0.811046
124a -> 127a: 0.048860
125a -> 127a: 0.030254
125a -> 130a: 0.015763

CyS-NEt$_2$:

Excitation energies and oscillator strengths:

Excited State 1: Singlet-A 2.0033 eV 618.90 nm f=1.1580
<S**2>=0.000
130 ->131 0.70726
This state for optimization and/or second-order correction.
Total Energy, E(TD-HF/TD-KS) = -1750.38708308
Copying the excited state density for this state as the 1-particle RhoCI density.

Excited State 2: Singlet-A 2.6171 eV 473.74 nm f=0.1071
<S**2>=0.000
129 ->131 0.69207

Excited State 3: Singlet-A 3.3065 eV 374.97 nm f=0.0063
<S**2>=0.000
126 ->131 0.12473
128 ->131 0.63939
130 ->132 0.25610

Excited State 4: Singlet-A 3.5347 eV 350.76 nm f=0.1506
<S**2>=0.000
126 ->131 0.16437
127 ->131 -0.33873
128 ->131 -0.26508
130 ->132 0.51744
130 ->133 0.10650

TD-DFT EXCITED STATES (TRIPLETS)
the weight of the individual excitations are printed if larger than 0.01

STATE 1: E= 0.040397 au 1.099 eV 8866.1 cm**$^{-1}$
128a -> 130a: 0.016725
129a -> 130a: 0.966327

STATE 2: E= 0.067148 au 1.827 eV 14737.3 cm**$^{-1}$
128a -> 130a: 0.932997
129a -> 130a: 0.015962
129a -> 131a: 0.021097

STATE 3: E= 0.095584 au 2.601 eV 20978.3 cm**$^{-1}$
126a -> 130a: 0.021495
126a -> 131a: 0.015152
127a -> 130a: 0.272145
128a -> 130a: 0.012368
129a -> 131a: 0.585325

STATE 4: E= 0.098682 au 2.685 eV 21658.1 cm**$^{-1}$
127a -> 130a: 0.611425
128a -> 131a: 0.015644
129a -> 131a: 0.299569

CySe-NEt$_2$:

Excitation energies and oscillator strengths:

Excited State 1: Singlet-A 1.9733 eV 628.31 nm f=1.1557
<S**2>=0.000
139 ->140 0.70807
This state for optimization and/or second-order correction.
Total Energy, E(TD-HF/TD-KS) = -3751.58189467
Copying the excited state density for this state as the 1-particle RhoCI density.

Excited State 2: Singlet-A 2.5397 eV 488.18 nm f=0.0703
<S**2>=0.000
138 ->140 0.69394

Excited State 3: Singlet-A 3.2292 eV 383.95 nm f=0.0220
<S**2>=0.000
137 ->140 0.65717

139 ->141 0.23012

Excited State 4: Singlet-A 3.5278 eV 351.44 nm f=0.0968 <S**2>=0.000

136 ->140 0.47288
137 ->140 0.20111
139 ->141 -0.46314

TD-DFT EXCITED STATES (TRIPLETS)
the weight of the individual excitations are printed if larger than 0.01

STATE 1: E= 0.039591 au 1.077 eV 8689.3 cm**$^{-1}$
137a -> 139a: 0.016524
138a -> 139a: 0.966859

STATE 2: E= 0.065372 au 1.779 eV 14347.5 cm**$^{-1}$
137a -> 139a: 0.937802
138a -> 139a: 0.015579
138a -> 140a: 0.019569

STATE 3: E= 0.093128 au 2.534 eV 20439.2 cm**$^{-1}$
132a -> 139a: 0.017330
135a -> 139a: 0.022341
135a -> 140a: 0.023494
136a -> 139a: 0.714628
138a -> 140a: 0.161982

STATE 4: E= 0.098323 au 2.676 eV 21579.4 cm**$^{-1}$
136a -> 139a: 0.189146
137a -> 139a: 0.015229
137a -> 143a: 0.014135
138a -> 140a: 0.724200

References

[1] *Chem. Commun.*, **2018**, 54, 11590-11593
[2] *Angew. Chem. Int. Ed.*, **2021**, 60, 18860-18866
[3] *Chem. Commun.*, **2019**, 55, 648-651
[4] Chem. Commun., **2017**, 53, 6117-6120
[5] *Color. Technol.*, **2019**, 135, 305-311
[6] *ACS Appl. Mater. Interfaces* **2018**, 10, 44324-44335
[7] *J. Am. Chem. Soc.* **2021**, 143, 49, 20828-20836